Onecut factors and Pou2f2 regulate diversification and migration of V2 interneurons in the mouse developing spinal cord

Audrey Harris[1], Gauhar Masgutova[1], Amandine Collin[1], Mathilde Toch[1], Maria Hidalgo-Figueroa[1,4], Benvenuto Jacob[2], Lynn M. Corcoran[3], Cédric Francius[1,5] and Frédéric Clotman[1*]

[1] Université catholique de Louvain, Institute of Neuroscience, Laboratory of Neural Differentiation, Brussels, Belgium; [2] Université catholique de Louvain, Institute of Neuroscience, System and Cognition division, Brussels, Belgium; [3] The Walter and Eliza Hall Institute, Molecular Immunology Division and Immunology Division, Parkville, Victoria, Australia.

For correspondence : frederic.clotman@uclouvain.be

[4] Present address : Neuropsychopharmacology & Psychobiology Research Group, Area of Psychobiology, Department of Psychology, University of Cadiz, Spain; Instituto de Investigación e Innovación en Ciencias Biomédicas de Cádiz (INiBICA), Spain

[5] Present address : PAREXEL International, France

Abstract

Acquisition of proper neuronal identity and position is critical for the formation of neural circuits. In the embryonic spinal cord, cardinal populations of interneurons diversify into specialized subsets and migrate to defined locations within the spinal parenchyma. However, the factors that control interneuron diversification and migration remain poorly characterized. Here, we show that the Onecut transcription factors are necessary for proper diversification and migration of the spinal V2 interneurons in the developing spinal cord. Furthermore, we uncover that these proteins restrict and moderate the expression of spinal isoforms of *Pou2f2*, a transcription factor known to regulate B-cell differentiation. By gain- or loss-of-function experiments, we show that Pou2f2 contribute to regulate the distribution of V2 populations in the developing spinal cord. Thus, we uncovered a genetic pathway that regulates the diversification and the migration of V2 interneurons during embryonic development.

Introduction

Neuronal migration is a critical feature of CNS development. It enables neurons, which initiate differentiation in the vicinity of the ventricular zone wherein neural progenitors are located, to reach adequate location in the nervous parenchyma and properly integrate into neural circuits. The mechanisms that regulate neuronal migration have been extensively studied in the developing brain, particularly for cortical interneurons (INs) that are produced in the ganglionic eminences and undergo a long tangential displacement to invade the cortex and integrate into cortical circuits (Barber and Pierani 2016, Guo and Anton 2014). In contrast, the factors that control IN migration in the developing spinal cord remain almost totally unknown.

In the embryonic spinal cord, distinct neuronal populations are generated from different progenitor domains orderly distributed along the dorsoventral axis of the ventricular zone. These progenitors produce motor neurons and multiple populations of ventral or dorsal INs (Lai, Seal, and Johnson 2016, Lu, Niu, and Alaynick 2015). In contrast to motor neurons, spinal IN populations do not organize into columns along the anteroposterior axis of the spinal cord (Francius et al. 2013). Nevertheless, they each migrate according to a stereotyped pattern and settle down at specific focused or diffuse locations in the spinal parenchyma (Grossmann et al. 2010). Recent studies demonstrated that proper neuronal distribution is critical for adequate formation of spinal circuits. Indeed, the clustering and dorsoventral settling position of motor neuron pools critically pattern sensory input specificity (Surmeli et al. 2011). Position of dorsal INs along the mediolateral axis in lamina V determines their connectivity with sensory afferents (Hilde et al. 2016) while extensor and flexor premotor INs segregate along the medio-lateral axis of the spinal cord (Tripodi, Stepien, and Arber 2011). Positional distinctions among premotor INs additionally correlate with their output to different motor columns (Goetz, Pivetta, and Arber 2015) and differential distribution of V1 IN subsets constrain patterns of input from sensory and from motor neurons (Bikoff et al. 2016). Consistently, distinct ventral IN subsets are differentially distributed along the anteroposterior axis of the spinal cord (Francius et al. 2013, Hayashi et al. 2018) and integrate into specific local microcircuit modules (Hayashi et al. 2018). However, the molecular mechanisms that regulate proper distribution of spinal INs remain elusive.

During their migration, cardinal populations of spinal neurons undergo progressive diversification into distinct subsets that exert specific functions in spinal circuits (Catela, Shin, and Dasen 2015, Lai, Seal, and Johnson 2016, Lu, Niu, and Alaynick 2015). For example, V2 INs diversify into major V2a and V2b and minor V2c and V2d populations. V2a and V2d are excitatory neurons that participate in left-right alternation at high speed and contribute to rhythmic activation of locomotor circuits, respectively (Crone et al. 2008, Dougherty and Kiehn 2010, Dougherty et al. 2013). V2b cells are inhibitory INs that participate in alternation of flexor vs extensor muscle contraction (Britz et al. 2015). As observed for V1 INs (Bikoff et al. 2016), V2 cells further diversify into more discrete subpopulations differentially distributed along the anteroposterior axis of the spinal cord (Francius et al. 2013, Hayashi et al. 2018). However, specific functions of these IN subsets have not been investigated yet, and the mechanisms that govern their production remain currently unknown.

Recently, we identified Onecut (OC) transcription factors as regulators of neuronal diversification (Kabayiza et al. 2017, Roy et al. 2012, Francius and Clotman 2014) and of dorsal IN migration (Kabayiza et al. 2017) in the developing spinal cord. OC factors, namely Hepatocyte Nuclear Factor-6 (HNF-6, or OC-1), OC-2 and OC-3, are transcriptional activators present in the digestive tract and in the CNS during embryonic development (Jacquemin et al. 1999, Lemaigre et al. 1996, Jacquemin et al. 2003, Landry et al. 1997, Vanhorenbeeck et al. 2002). In neural tissue, they regulate production (Espana and Clotman 2012a), diversification (Roy et al. 2012, Francius and Clotman 2014, Kabayiza et al. 2017), distribution (Audouard et al. 2013, Espana and Clotman 2012a, b, Kabayiza et al. 2017) and maintenance (Espana and Clotman 2012a, b, Stam et al. 2012) of specific neuronal populations, as well as the formation of neuromuscular junctions (Audouard et al. 2012). Here, we demonstrate that OC factors regulate the diversification and the distribution of V2 INs during spinal cord development. Analyzes of OC-deficient embryos showed defective production of specific subpopulations of V2a INs, as well as abnormal distribution of V2a and V2b cells in the developing spinal cord. Furthermore, we uncovered that OC proteins act upstream of specific spinal isoforms of Pou2f2, a POU family transcription factor. Using gain- or loss-of-function experiments, we demonstrated that, as observed for OC factors, Pou2f2 regulates the distribution of V2 INs in the developing spinal cord. Thus, we uncovered a genetic pathway that regulates the diversification and the migration of V2 INs during embryonic development.

Results

OC factors are present in multiple subsets of spinal V2 interneurons

In the developing spinal cord, OC factors contribute to diversification, migration and maintenance of different neuronal populations (Kabayiza et al. 2017, Roy et al. 2012, Stam et al. 2012). To study V2 interneuron diversification, we previously established a repertoire of markers that divide embryonic V2 cells into multiple subpopulations (Francius et al. 2013). Although OC factors have been detected in V2 interneurons (Francius and Clotman 2010), their distribution in V2 subsets has not been investigated yet. Therefore, we first determined the presence of each OC in these V2 subpopulations at e12.5.

V2a interneurons include neuronal subsets characterized by the presence of Shox2, MafA, cMaf, Bhlhb5 or Prdm8 (Francius et al. 2013). Only Hnf6 was detected in few Shox2+ V2a cells (Figure 1A-C"; Table 1). In contrast, the 3 OC proteins were detected in MafA+ and cMaf+ V2a subpopulations (Figure 1D-I"; Table 1), but not in Bhlhb5+ or Prdm8+ cells (Table 1; data not shown). V2b interneurons include similar subsets except for Shox2+ and cMaf+ cells, and contain an additional MafB+ subpopulation (Francius et al. 2013). OC were present in MafA+ but not in MafB+, Bhlhb5+ or Prdm8+ V2b subsets (Figure 1J-L"; Table 1; data not shown). In addition, OC were detected in V2c (non-progenitor Sox1+ cells; Figure 1M-O"; Table 1) but not in V2d (Shox2+Chx10-) cells (Figure 1A-C"; Table 1). Thus, OC factors are present in multiple subpopulations of V2 interneurons.

V2 – e12.5				
Populations	**Subpopulations**	**HNF-6**	**OC-2**	**OC-3**
V2a – Chx10		+	+	+
	Shox2	+	-	-
	MafA	+	+	+
	cMaf	+	+	+
	Bhlhb5	-	-	-
	Prdm8	-	-	-
V2b – Gata3		+	+	+
	MafA	+	+	+
	MafB	-	-	-
	Bhlhb5	-	-	-
	Prdm8	-	-	-
V2c – Sox1		+	+	+
V2d – Shox2		-	-	-

137

138 **Table 1. OC factors are present in specific populations and subpopulations of V2**
139 **interneurons.** The V2 populations, including V2a, V2b, V2c and V2d, are subdivided in
140 smaller subpopulations characterized by differential expression of transcription factors
141 (Francius et al. 2013). OC factors are detected in specific populations and subpopulations of
142 V2 interneurons.

143

144

145 **OC factors regulate the diversification of spinal V2 interneurons**

146 To determine whether OC proteins contribute to the development of V2 interneuron
147 subsets, we characterized the phenotype of these cells in *Hnf6/Oc2* double-mutant embryos,
148 which lack the three OC factors in the developing spinal cord (Kabayiza et al. 2017, Roy et al.
149 2012). Given that the number and the distribution of cells in each interneuron subpopulation
150 vary along the anteroposterior axis of the spinal cord (Francius et al. 2013, Hayashi et al.
151 2018, Sweeney et al. 2018), this analysis was systematically performed at brachial, thoracic
152 and lumbar levels at e12.5 and e14.5.

153 In the absence of OC factors, the total number of Chx10+ interneurons was not significantly
154 changed (Figure 2A-D; Supplementary Figure S1A-B), although a trend toward reduction was
155 detected at brachial level at e12.5 (Figure 2C). A large subset of V2a cells contains Shox2
156 (Figure 1A-C"; 2E-F"; (Dougherty et al. 2013)). Consistently, the number of Chx10+Shox2+
157 interneurons was not changed in the absence of OC proteins (Figure 2E-H; Supplementary
158 Figure S1C-D"). These observations suggest that OC are not necessary for V2a interneuron
159 production. In contrast, the smaller V2a subpopulations wherein OC factors were detected
160 in control embryos, characterized by the presence of MafA (Figure 1D-F") or cMaf (Figure
161 1G-I"), were almost completely lost in OC mutant embryos (Figure 2I-P; Supplementary
162 Figure S1E-H"). As the total number of Chx10+ and of Shox2+ V2a was not changed (Figure
163 2A-H; Supplementary Figure S1A-D"), the loss of the MafA+ or cMaf+ subsets may be
164 compensated for by expansion of other V2a subpopulations. However, we were unable to
165 detect expansion of any alternative V2a subset (data not shown), suggesting that the
166 absence of OC proteins favor differentiation of V2a subpopulations that remain to be
167 identified. Nevertheless, our data indicate that OC factors are required either for the
168 expression of V2 subpopulation markers or for the differentiation of specific V2a
169 interneuron subsets.
170 To discriminate between these possibilities and to evaluate the contribution of OC factors to
171 V2b diversification, we characterized the phenotype of V2b interneurons and of their MafA+
172 subpopulation in the absence of OC proteins. As observed for V2a interneurons, the total
173 number of V2b cells was not changed in OC mutant embryos (Figure 2Q-T; Supplementary
174 Figure S1I-J), although a trend toward reduction was observed at brachial level at e12.5
175 (Figure 2S). As for V2a, OC are present in the MafA+ V2b subpopulation (Figure 1J-L").
176 However, in contrast to V2a, the MafA+ V2b interneurons were present in normal number in
177 OC mutant embryos (Figure 2U-X; Supplementary Figure S1K-L''). Hence, OC factors are not
178 necessary for *MafA* expression in spinal V2 interneurons nor for the production of the
179 MafA+ V2b subset, although they are required for the differentiation of the MafA+ and of
180 the cMaf+ V2a subpopulations.
181 Finally, we assessed the requirement for OC in the production of V2c interneurons, a V2
182 population strongly related to V2b cells (Panayi et al. 2010) wherein OC are broadly present
183 (Figure 1M-O"). Although weak production of Sox1 in spinal progenitors was preserved, V2c
184 cells characterized by high Sox1 levels were scarcely detectable in OC mutant embryos at

185 e12.5 (arrows in Figure 2Y-AA). However, the number of V2c was normal at e14.5 (Figure
186 2BB; Supplementary Figure S1M-N), suggesting that the absence of OC delays the
187 differentiation of V2c interneurons without affecting the V2b population. Taken together,
188 these observations demonstrate that OC proteins are not required for V2 interneuron
189 production but regulate the diversification of V2 interneurons into multiple subpopulations.
190
191 **OC factors regulate the distribution of spinal V2 interneurons**
192 Although the total number of V2a or V2b interneurons was not affected by the absence of
193 OC factors, careful examination of immunofluorescence labelings suggested that, as
194 observed for spinal dorsal interneurons (Kabayiza et al. 2017), OC proteins may regulate the
195 distribution of V2 interneurons in the developing spinal cord (Figure 2A-B; Q-R). Therefore,
196 quantitative distribution analyses (Kabayiza et al. 2017) were performed for each V2
197 population present in OC mutant embryos at brachial, thoracic or lumbar levels at e12.5,
198 namely in the course of ventral interneuron migration, and at e14.5, i.e. when ventral
199 interneuron migration in the transverse plane of the spinal cord is completed.
200 At e12.5 in control embryos, V2a interneurons distributed in 2 connected clusters, a major
201 central group and a minor medial group, at each level of the spinal cord. In mutant embryos,
202 V2a cells similarly distributed in connected central and medial groups. However, the relative
203 cell distribution between the 2 clusters seemed altered, with less central cells at brachial
204 level and less medial cells at lumbar levels (Figure 3A-L). Altered V2a distribution on the
205 mediolateral axis was confirmed at e14.5. In control embryos, the 2 V2a groups did coalesce
206 in a more evenly-distributed population that occupied ~70% of the medio-lateral axis. In
207 mutant embryos, V2a interneurons remained segregated into 2 distinct, although
208 connected, clusters with a majority of cells in medial position (Figure 3M-X). Thus, absence
209 of OC factors perturbs proper distribution of the V2a interneurons and restricts at e14.5
210 migration of a fraction of V2a cells in a medial position. To assess whether these distribution
211 defects may only affect V2a subsets or impact the whole V2a population, we sought to
212 characterize the distribution of V2a subpopulations. However, the MafA+ and cMaf+ subsets
213 were absent in OC mutants. Therefore, only the broader Shox2+ subpopulation was
214 analyzed. Similar observations were made as for the whole V2a population (Figure 3Y-VV),
215 confirming that absence of OC factors alters the distribution of V2a interneurons.

216 To assess whether OC also regulate the position of other V2 populations, we studied the
217 distribution of V2b interneurons. At e12.5 in control embryos, V2b cells distributed in a
218 major central (brachial level) or lateral (thoracic and lumbar levels) cluster with minor
219 subsets located more medially (arrows in Figure 4A-L) or ventrally (arrowheads in Figure 4A-
220 L). In OC mutant embryos at e12.5, the major population was more compact, more centrally
221 located and slightly more ventral. In addition, the ventral V2b subset was significantly
222 depleted (asterisks in Figure 4A-L). Consistently, at e14.5, V2b interneurons in the central
223 cluster remained significantly more compact at brachial level in the absence of OC factors,
224 and identical trends were observed at thoracic and lumbar levels (Figure 4M-X). In addition,
225 a small contingent of V2b migrating towards the medio-dorsal spinal cord in control embryos
226 (arrowheads in Figure 4M-X) was missing in OC mutant littermates (asterisks in Figure 4M-X).
227 Thus, as observed for V2a cells, absence of OC factors perturbs proper distribution of the
228 V2b interneurons. The MafA+ V2b subset was too small to enable reliable distribution
229 analysis. Taken together, these observations demonstrate that, in addition to V2
230 diversification, the OC transcription factors regulate proper distribution of V2 interneurons
231 during spinal cord development.
232
233 **OC factors control expression of neuronal-specific isoforms of *Pou2f2***
234 In an effort to identify genes downstream of OC that may contribute to V2 interneuron
235 differentiation and distribution, we performed a microarray comparison of control and of
236 OC-deficient spinal cord transcriptome at e11.5, namely at the stage when significant
237 numbers of V2 cells have been generated and are initiating migration. Among genes showing
238 a differential expression level in the OC mutant spinal cord, *Pou2f2* was significantly
239 upregulated (1.57-fold increase). Pou2f2 (previously named Oct-2) is a transcription factor
240 containing a POU-specific domain and a POU-type homeodomain (Figure 5A) that binds an
241 octamer motif (consensus sequence ATGCAAAT) (Latchman 1996). *Pou2f2* expression has
242 been detected in B lymphocytes, in neuronal cell lines and in neural tissues including the
243 developing CNS (Lillycrop and Latchman 1992, Camos et al. 2014, Hatzopoulos et al. 1990).
244 Pou2f2 is required for differentiation of B lymphocytes and for postnatal survival (Corcoran
245 et al. 1993, Corcoran et al. 2004, Hodson et al. 2016, Konig et al. 1995), and is able to
246 modulate neuronal differentiation of ES cells (Theodorou et al. 2009). However, its role in
247 the developing spinal cord remains unknown.

248 Based on work in B cells, multiple *Pou2f2* isoforms generated by alternative splicing have
249 been described (Figure 5A; (Lillycrop and Latchman 1992, Wirth et al. 1991, Hatzopoulos et
250 al. 1990, Liu, Lillycrop, and Latchman 1995, Stoykova et al. 1992)). Therefore, we first
251 determined whether similar isoforms are found in the developing spinal cord. However,
252 using RT-PCR experiments, we systematically failed to obtain PCR products using upstream
253 primers in described exon 1 (asterisks in Supplementary Figure S2A-B and data not shown;
254 Table 2) and amplifications encompassing exons 5 to 6 generated predominant amplicons
255 larger than expected (arrowheads in Supplementary Figure S2B; Table 2), suggesting the
256 existence of alternative exons in *Pou2f2* embryonic spinal cord transcripts (Figure 5A). Data
257 mining the NCBI Nucleotide database for *Pou2f2* sequences identified a predicted murine
258 *Pou2f2* isoforms (X6 sequence, accession number XM_006539651.3) with a different exon 1
259 (E1X) and an additional sequence between exons 5 and 6, the size of which (279 bp)
260 corresponded to the size differences estimated in our amplifications encompassing exons 5
261 to 6 (arrowheads in Supplementary Figure S2B; Table 2). Using PCR primers in this predicted
262 sequence, we were able to amplify a 5' region of *Pou2f2* from the alternative E1X exon and
263 an additional sequence between exons 5 and 6 (Supplementary Figure S2C; Table 2),
264 suggesting that alternative isoforms similar to this predicted sequence are produced in the
265 developing spinal cord. However, amplifications from E1X systematically produced 2
266 amplicons (arrowheads in Supplementary Figure S2C; Table 2), suggesting the existence of
267 an alternative exon downstream to E1X. Sequencing of our PCR products and alignment to
268 genomic DNA confirmed that predominant *Pou2f2* isoforms in the developing spinal cord
269 contain the alternative E1X exon, an additional exon (E5b) between exons 5 and 6, and can
270 undergo alternative splicing of a short (61bp) exon (E1b) between E1X and exon 2
271 (Supplementary Figure S2D). E5b exon maintains the reading frame. In contrast E1b exon
272 disrupts the reading frame, imposing the use of the ATG located in exon 2 to generate a
273 functional Pou2f2 protein, whereas the absence of E1b leaves open the use of an alternative
274 upstream ATG located at the 3' end of E1X (Figure 5A; Supplementary Figure S2D). Hence,
275 taking into account our RT-PCR and sequencing data, 4 neuronal *Pou2f2* isoforms that are
276 different from the previously described B-cell or neural isoforms can be produced in the
277 developing spinal cord (Fig 5A).
278 However, our RT-PCR experiments suggested that minor transcripts corresponding to B-cell
279 isoforms are also present in the embryonic spinal cord (Supplementary Figure S2A-B; Table

280 2). To assess the relative abundance of each transcript type in this tissue and to evaluate the
281 extent of their relative overexpression in the absence of OC factors, we quantified each
282 isoform type in control and in OC-deficient spinal cord at e11.5. In control spinal cords,
283 spinal *Pou2f2* isoforms were >30-fold more abundant than B-cell isoforms (Figure 5B),
284 consistent with our RT-PCR observations (Supplementary Figure S2). In the absence of OC
285 factors, spinal isoforms were ~2.6-fold overexpressed whereas B-cell isoforms barely
286 trended to increase (Figure 5C-D), resulting in spinal isoforms being >60-fold more abundant
287 than B-cell transcripts (Figure 5E). Thus, OC factors repress expression of spinal *Pou2f2*
288 isoforms in the developing spinal cord.
289 To confirm these data and to determine the expression pattern of *Pou2f2* in the ventral
290 spinal cord, *in situ* hybridization was performed on sections from control or *Hnf6/Oc2*
291 double-mutant spinal cords using either a generic *Pou2f2* probe complementary to spinal
292 and to B-cell isoforms or a spinal isoform-specific probe corresponding only to exon E5b
293 (Figure 5A). Using the generic *Pou2f2* probe on control tissue, we detected *Pou2f2*
294 transcripts in the ventral region of the spinal cord, with lower expression levels in the
295 location of the motor columns (arrows in Figure 5F). In OC mutant embryos, *Pou2f2*
296 expression was globally increased and additionally expanded in the ventral area (arrowheads
297 in Figure 5F-G) including the motor neuron territories (arrows in Figure 5F-G). Similar
298 observations were made with the spinal-specific probe, although the signal was much
299 weaker probably owing to the shorter length of the probe (Figure 5H-I). Thus, OC factors
300 restrict and moderate *Pou2f2* expression in ventral spinal populations likely including V2
301 interneurons.
302
303
304
305
306
307
308
309
310

Amplification	Expected sizes	B cells	Control spinal cord
E1 → E6	272 bp 390 bp 456 bp	272 bp 390 bp 456 bp	No amplification
E7 → E9	174 bp 222 bp	174 bp 222 bp	174 bp
E10 → E12	452 bp	452 bp	452 bp
E13 → E17	160 bp 296 bp 370 bp	160 bp 296 bp 370 bp	370 bp
E1 → E7	348bp 466 bp 532 bp	466 bp 532 bp	No amplification
E2 → E7	284 bp 402 bp 468 bp	402 bp 468 bp	~ 680 bp ~ 750 bp
E3 → E6	154 bp 272 bp 378 bp	154 bp 272 bp 378 bp	272 bp 378 bp ~ 550 bp ~ 600 bp
E4 → E7	340 bp	340 bp	~ 600 bp
E5 → E7	201 bp	201 bp	201 bp ~ 460 bp
E6 → E7	160 bp	160 bp	160 bp
E1X → E3	152 bp	No amplification	152 bp ~ 220 bp
E1X → E5b	554 bp 620 bp	N.D	554 bp 620 bp
E5b	234 bp	N.D	234 bp
E3 → E5b	429 bp 495 bp	N.D	429 bp 495 bp
E5b → E7	416 bp	N.D	416 bp

311 **Table 2. *Pou2f2* isoforms in the developing spinal cord are different from B-cell isoforms.**
312 Regions covering B lymphocytes or predicted *Pou2f2* isoforms (exons E1 or E1X to E17) were
313 amplified by RT-PCR from B lymphocyte or embryonic spinal cord RNA. Orange cells =
314 unexpected results.
315
316
317 **Pou2f2-positive V2 interneurons are mislocated in the absence of OC factors**
318 To assess whether increased *Pou2f2* expression in *Hnf6*$^{-/-}$;*Oc2*$^{-/-}$ spinal cords corresponded to
319 an expansion of Pou2f2 distribution in V2 interneurons or an upregulation in its endogenous
320 expression territory, we first quantified the number and distribution of Pou2f2-containing
321 Chx10+ cells at e12.5 and e14.5 (Figure 6; Supplementary Figure S3). Immunofluorescence
322 experiments demonstrated that Pou2f2 is present in V2a interneurons in control embryos
323 (Figure 6A,C; Supplementary Figure S3A,D). They also confirmed increased Pou2f2
324 production in the ventral regions of the spinal cord in OC mutant embryos (Figure 6A-F).
325 However, the increase in Pou2f2-positive V2a interneurons was not statistically significant
326 (Figure 6E-F; Supplementary Figure S3). This suggested that, in the absence of OC factors,
327 *Pou2f2* is upregulated but only modestly expanded in the V2a population. In contrast, the
328 distribution of Pou2f2-positive V2a interneurons was affected (Figure 6A-D, 6G-DD). At
329 e12.5, cells in the central clusters were slightly reduced at brachial and at thoracic levels
330 (Figure 6G-R). In contrast, at e14.5, a majority of V2a containing Pou2f2 settled in a medial
331 position (Figure 6S-DD), reminiscent of the distribution defects observed for the whole V2a
332 population (Figure 3). Similarly, Pou2f2 was detected in V2b interneurons in control
333 embryos, although in a more restricted number of cells (Figure 7A-F). In the absence of OC
334 factors, the number of Pou2f2-positive V2b cells was not significantly increased (Figure 7E-F)
335 but, as observed for V2a, this subset of V2b interneurons was slightly mislocated with cells
336 more central at e12.5 and more clustered on the medio-lateral axis at e14.5 (Figure 7G-DD).
337 Taken together, these observations suggest that Pou2f2 may contribute to control V2
338 interneuron migration during spinal cord development and that increased *Pou2f2* expression
339 in these cells could participate in alterations of V2 distribution in the absence of OC factors.
340
341
342

343 **Pou2f2 regulates the distribution of spinal V2 interneurons**

344 To determine whether Pou2f2 is able to modulate V2 interneuron distribution, we expressed
345 *Pou2f2*, which is not present in the chicken genome (data not shown), in the chicken
346 embryonic spinal cord (Supplementary Figure S4). Pou2f2 did not impact on the number of
347 V2a, Shox2-containing V2a, V2b or V2d interneurons (Figure 8A-B", 8K-P). In contrast, it did
348 alter V2 interneuron location. In HH27-28 control spinal cord, V2a and Shox2-containing V2a
349 interneurons were distributed in 2 closely connected clusters on the medio-lateral axis of
350 the neuroepithelium. In electroporated spinal cord, lateral migration was increased and a
351 majority of V2a and Shox2-positive V2a interneurons were clustered in a single group in a
352 central position (Figure 8A-J) with ectopic lateral extensions (arrows in Figure 8D,H). In
353 control spinal cord, V2b were distributed in 2 groups along the medio-lateral axis with a
354 majority of cells in the lateral cluster. In electroporated spinal cord, lateral migration of the
355 V2b interneurons was reduced and a majority of cells were located in the medial cluster
356 (Figure 8O-T). Thus, consistent with our observation in OC mutant embryos, increased
357 Pou2f2 seems to modulate migration of V2 interneurons in the developing spinal cord.

358 To confirm the influence of Pou2f2 on V2 migration, we studied V2 distribution in mouse
359 embryos devoid of Pou2f2 (Corcoran et al. 1993) at e12.5. Absence of Pou2f2 did not impact
360 on the number of V2a, Shox2-positive V2a or V2d interneurons (Figure 9A-G) nor on the
361 cMaf+ or Maf+ V2a subsets (Supplementary Figure S5). In contrast, V2a distribution was
362 affected in *Pou2f2* mutants. As compared to the two V2a clusters observed in control
363 embryos, Chx10+ cells were relatively more abundant in the medial cluster in *Pou2f2* mutant
364 embryos (Figure 9H-S). Similarly, Shox2+ V2a remained more medial at brachial level, but
365 migrated more laterally at lumbar level (Figure 9T-EE). Consistent observations were made
366 for V2b and V2c interneurons (Figure 10). Although the number of V2b, V2c or MafA+ V2b
367 cells was not changed in the absence of Pou2f2 (Figure 10A-C; Supplementary Figure S6),
368 V2b cells remained more medial at thoracic levels but migrated more laterally at lumbar
369 levels (Figure 10D-O). Taken together, these observations demonstrate that Pou2f2 regulate
370 the distribution of V2 interneurons during spinal cord development.

371

372

373 **Discussion**

374

375 In the recent years, several studies demonstrated that proper distribution of neuronal
376 populations and subpopulations in the developing spinal cord is critical for adequate
377 formation of spinal circuits (Bikoff et al. 2016, Goetz, Pivetta, and Arber 2015, Hayashi et al.
378 2018, Hilde et al. 2016, Surmeli et al. 2011, Tripodi, Stepien, and Arber 2011). However, the
379 genetic programs that control the diversification of spinal neuronal populations into
380 specialized subpopulations and the proper settling of these neuronal subsets in the spinal
381 parenchyma remain elusive. Here, we provide evidence that OC transcription factors
382 regulate the diversification of spinal V2 INs, and that a genetic cascade involving OC factors
383 and their downstream target Pou2f2 controls the distribution of V2 INs in the developing
384 spinal cord.

385

386 **Control of V2 IN diversification by the OC factors**

387 Cardinal populations of spinal ventral INs have been well characterized, and their global
388 contribution to the activity of motor circuits has been extensively studied (reviewed in (Boije
389 and Kullander 2018, Gosgnach et al. 2017, Ziskind-Conhaim and Hochman 2017). However,
390 more recently, the idea emerged that these cardinal populations are not homogeneous
391 ensembles but rather contain multiple cellular subsets with distinct molecular identities and
392 functional properties. V0 INs are constituted of two major populations, the inhibitory $V0_D$
393 and the excitatory $V0_V$ neurons, which control left-right alternation of motor circuit
394 activation at low or high frequencies, respectively (Talpalar et al. 2013). V1 INs, a major
395 inhibitory population that controls motor output, can be fractionated into ~50 distinct
396 subsets based on the combinatorial expression of 19 transcription factors. These subsets
397 exhibit distinct electrophysiological properties and highly structured spatial distribution that
398 constraints somato-sensory afferences (Bikoff et al. 2016). Furthermore, they are
399 differentially distributed along the anteroposterior axis of the spinal cord (Francius et al.
400 2013, Sweeney et al. 2018), suggesting differential contribution to the motor output at
401 thoracic or at limb levels of the spinal cord (Sweeney et al. 2018). Similarly, V2a INs comprise
402 two major divisions, namely type I and type II V2a cells, that are arrayed in counter-gradients
403 along the antero-posterior axis of the spinal cord and activate different patterns of motor
404 output at brachial and lumbar levels. Furthermore, these two large divisions can themselves

405 be fractionated at birth into 11 subsets characterized by distinct combinations of markers,
406 differential segmental localization and specific distribution patterns on the medio-lateral axis
407 of the spinal cord (Hayashi et al. 2018). In the zebrafish, 3 distinct subclasses of V2a INs
408 participate in separate microcircuit modules driving slow, intermediate or fast motor neuron
409 activity (Ampatzis et al. 2014). Finally, V3 INs segregate into physiologically and
410 topographically distinct clusters along the dorso-ventral axis of the spinal cord, each showing
411 distinctive maturation processes and likely playing different roles in motor activity
412 (Borowska et al. 2015, Borowska et al. 2013). Taken together, these observations suggest
413 that cardinal IN populations only constitute the first organization level of functionally distinct
414 neuronal subsets that contribute to diversity and flexibility within spinal motor circuits. We
415 show here that, as observed in spinal motor neurons and other IN populations (Francius and
416 Clotman 2010, Francius et al. 2013, Kabayiza et al. 2017), OC factors are also detected in
417 subsets of V2 INs. As reported for the V1 population (Bikoff et al. 2016, Sweeney et al. 2018),
418 OC proteins may define functionally-relevant V2 subpopulations, although possible
419 correlation with the recently-identified V2a subsets (Hayashi et al. 2018) remains to be
420 investigated.
421 However, for each of these cardinal populations, the genetic programs that contribute to
422 their diversification into multiple subpopulations remain unknown. Our observations
423 demonstrate that OC factors contribute to the diversification of V2 INs. Normal numbers of
424 cardinal V2a and V2b cells were generated in OC mutant embryos, suggesting that these
425 factors do not contribute to the production of V2 cells (Clovis et al. 2016, Lee et al. 2008,
426 Thaler et al. 2002) nor to the segregation of the V2a and V2b lineages through differential
427 activation of Notch signaling (Del Barrio et al. 2007, Joshi et al. 2009, Misra et al. 2014, Peng
428 et al. 2007). In contrast, V2a subpopulations characterized by the presence of MafA or cMaf
429 were strongly depleted in the absence of OC proteins. Uncomplete knowledge of the whole
430 collection of V2a subsets prevented to assess whether this reduction in specific
431 subpopulations were compensated for by an expansion of neighboring subsets.
432 Furthermore, MafA and cMaf were not included among the markers that fractionate at birth
433 the V2a population into 11 distinct subgroups (Hayashi et al. 2018) and the matching
434 between these subpopulations therefore remains to be investigated. Nevertheless, these
435 observations suggest that, as previously observed for spinal motor neurons (Roy et al. 2012)
436 and dorsal INs (Kabayiza et al. 2017), OC factors contribute to the diversification of V2a INs

437 during development. In addition, the production of V2c cells was delayed in OC mutant
438 embryos, although V2b that are supposed to constitute the source of V2c (Panayi et al.
439 2010) were timely generated. This points to a specific contribution of OC protein to the
440 development of V2c INs, the mechanism of which is currently unknown.
441
442 **Control of V2 IN migration by the OC factors**
443 Beside diversification, the characterization of functionally distinct IN subpopulations
444 unveiled a strong correlation between the distribution of each IN subset and their
445 contribution to distinct microcircuit modules. Extensor and flexor premotor INs segregate
446 along the medio-lateral axis of the spinal cord (Tripodi, Stepien, and Arber 2011). Premotor
447 INs that convey information to motor neurons innervating axial muscles reside in
448 symmetrically balanced locations while limb-innervating motor neurons are mainly
449 innervated by ipsilateral premotor INs (Goetz, Pivetta, and Arber 2015). The settling position
450 of distinct V1 IN subsets is predictive of the status of motor and sensory neuron input (Bikoff
451 et al. 2016). Among V2 INs, type I cells are distributed as an increasing rostro-caudal gradient
452 and contribute to local motor circuits, whereas type II cells are arrayed as an increasing
453 caudo-rostral gradient and project both to motor neurons and supraspinally (Hayashi et al.
454 2018), likely sending motor efference copies to the cerebellum via the lateral reticular
455 nucleus (Azim et al. 2014, Pivetta et al. 2014). Furthermore, ventral and dorsal V3 INs are
456 differentially activated during running and swimming, suggesting specific contribution of
457 spatially distinct V3 subsets to different motor behavior (Borowska et al. 2013). Finally,
458 inhibitory sensory relay neurons of lamina V characterized by the presence of SATB2 are
459 abnormally located upon *SATB2* inactivation and this, along with changes in molecular
460 identity, perturbs pre- and post-synaptic connectivity (Hilde et al. 2016). Taken together,
461 these recent data support a model wherein correct localization of spinal IN subsets is critical
462 for proper formation of sensory and sensory-motor circuits, reminiscent of the requirement
463 of correct motor neuron positioning for the establishment of adequate sensory inputs
464 (Surmeli et al. 2011, Dasen 2017). This highlights the importance of a strict regulation of
465 short-distance neuronal migration in the developing spinal cord.
466 However, genetic determinants that control spinal IN migration have only been sparsely
467 identified. Sim1 regulate ventro-dorsal migration of the V3 IN subsets (Blacklaws et al. 2015).
468 Similarly, SATB2 control the position of inhibitory sensory relay INs along the medio-lateral

469 axis of the spinal cord (Hilde et al. 2016). Here, we provide evidence that the OC factors
470 control a genetic program that regulates proper positioning of V2 INs during embryonic
471 development. In the absence of OC proteins, a fraction of V2a INs remained in a more
472 medial location, expanding the medial cluster containing locally-projecting cells at the
473 expanse of the lateral cluster that comprises the supraspinal-projecting V2a INs (Hayashi et
474 al. 2018). V2b alterations were less spectacular, although ventral and dorsal contingents
475 were reduced and the cell distribution in the central cluster was altered. Variability in the
476 alterations observed at e12.5 and e14.5 suggests that, depending on the population
477 considered, migration of earlier- or later-migrating neurons may be differently affected by
478 the absence of OC proteins. Functional distinctions between V2b subsets have not been
479 reported to date. However, given our current knowledge regarding the diversification and
480 the impact of localization of V1 and V2a IN subpopulations on proper circuit formation
481 (Bikoff et al. 2016, Hayashi et al. 2018), we hypothesize that even slight perturbations in the
482 distribution of small IN subsets are likely to result in alterations in spinal microcircuit
483 development. Our observations are consistent with the contribution of OC factors to the
484 migration of several populations of spinal dorsal INs (Kabayiza et al. 2017). This raises the
485 question whether similar cues might be regulated by identical genetic programs and used by
486 different IN populations to organize proper distribution of ventral and dorsal IN subsets in
487 the developing spinal cord. Identification of the factors downstream of OC protein involved
488 in the control of neuronal migration will be necessary to answer this question.
489
490 **A OC-Pou2f2 genetic cascade regulates the migration of V2 INs**
491 Therefore, we attempted to identify genes downstream of OC factors and possibly involved
492 in the control of IN migration using a global approach comparing the transcriptome of whole
493 spinal cords isolated from control or OC-deficient embryos. However, we were unable to
494 detect significant changes in the expression of known regulators of neuronal migration. This
495 suggests that different actors may be active downstream of OC proteins in distinct IN
496 subsets to regulate proper neuronal distribution. In contrast, we uncovered that expression
497 of the transcriptional regulator *Pou2f2* is repressed by OC factors in multiple IN populations.
498 Surprisingly, our data demonstrated that variant *Pou2f2* isoforms are produced in the
499 developing spinal cord as compared to B lymphocytes (Lillycrop and Latchman 1992, Wirth
500 et al. 1991, Hatzopoulos et al. 1990, Liu, Lillycrop, and Latchman 1995, Stoykova et al. 1992),

501 and that these spinal variants are regulated by OC proteins. Spinal-enriched transcripts
502 encode Pou2f2 proteins containing additional peptidic sequences upstream of the POU-
503 specific domain and of the homeodomain. Furthermore, exon 1 is different and corresponds
504 to sequences located ~47kb upstream of the transcription initiation site used in B cells (data
505 not shown) in the mouse genome, suggesting that OC regulate *Pou2f2* expression from an
506 alternative promoter. However, we cannot exclude that additional exon(s) could be present
507 upstream of the identified sequences, and determination of the regulating sequences
508 targeted by the OC protein will require thorough characterization of the produced
509 transcripts. In addition, we cannot rule out indirect regulation of *Pou2f2* expression by the
510 OC factors, as these proteins are usually considered to be transcriptional activators rather
511 than repressors (Beaudry et al. 2006, Jacquemin et al. 2000, Jacquemin, Lemaigre, and
512 Rousseau 2003, Lannoy et al. 2000, Pierreux et al. 2004, Roy et al. 2012). Whether divergent
513 N-terminal sequence and additional peptidic sequence upstream of the POU-specific domain
514 modifies the activity or the binding specificity of the Pou2f2 proteins also awaits further
515 investigations.
516 Nevertheless, our observations demonstrate that Pou2f2 is downstream of OC factors in the
517 V2 INs and also contributes to regulate the distribution of V2 INs during embryonic
518 development. The number of Pou2f2-containing V2 was not significantly increased in OC
519 mutant spinal cords, suggesting that the absence of OC protein resulted in derepression of
520 Pou2f2 production in its endogenous expression domain rather that ectopic activation in
521 other V2 subsets. Increased production of Pou2f2 in the chicken embryonic spinal cord
522 resulted in alterations in the localization of V2 populations without any change in cell
523 number, pointing to a possible contribution of Pou2f2 to the regulation of V2 migration
524 downstream of OC factors. Consistently, V2 distribution was perturbed in *Pou2f2* mutant
525 embryos without any alteration in V2 population or subpopulation cell numbers,
526 demonstrating the involvement of Pou2f2 in the control of V2 IN distribution. Hence, we
527 uncovered a genetic cascade comprising OC and Pou2f2 transcription factors that ensures
528 proper migration of V2 cells during spinal cord development. This program may not be
529 restricted to V2 cells, as diversification and distribution of dorsal INs and of motor neurons
530 are also altered in the absence of OC factors (Kabayiza et al. 2017, Roy et al. 2012) and as
531 *Pou2f2* expression in the OC mutant spinal cord is increased in multiple neuronal
532 populations (Figure 5D-I). Therefore, evaluating the consequences of V2 IN defects on motor

533 circuit activity in *OC* or *Pou2f2* mutants would necessitate conditional inactivation of these
534 transcription factors in this specific population. Whether V2 localization defects are
535 associated with axon guidance perturbations, as observed for V3 INs in the absence of Sim1
536 (Blacklaws et al. 2015), will require genetic labeling of V2 axonal projections.
537 Localization defects of specific neuronal populations have previously been reported in the
538 absence of OC factors. Dopaminergic neurons of the A13 nucleus migrate aberrantly in OC
539 mutant embryos, resulting in the disaggregation of the nucleus and loss of dopaminergic cell
540 phenotype (Espana and Clotman 2012b). Similarly, neurons of the Locus Coeruleus, the
541 largest noradrenergic nucleus of the CNS, migrate caudally beyond their normal position in
542 the rostral hindbrain of OC deficient individuals, resulting in the loss of their
543 catecholaminergic characteristics (Espana and Clotman 2012a). Final positioning of the
544 Purkinje cells during postnatal maturation of the cerebellum was defective in the absence of
545 HNF-6 (Audouard et al. 2013). Finally, distribution defects of spinal dorsal INs in OC mutant
546 embryos have recently been reported (Kabayiza et al. 2017). Hence, OC factors seem critical
547 for proper localization of multiple neuronal populations throughout the CNS. Whether
548 identical migration regulators are controlled by OC proteins in different neuronal
549 populations remains to be determined. Comparison of downstream targets of OC and of
550 Pou2f2 that would be oppositely regulated in the respective mutants may constitute a
551 strategy to identify these regulators.
552

553 **Materials and methods**

554

555 **Ethics statement and mouse lines**

556 All experiments were strictly performed in accordance with the European Community
557 Council directive of 24 November 1986 (86-609/ECC) and the decree of 20 October 1987 (87-
558 848/EEC). Mice were raised in our animal facilities and treated according to the principles of
559 laboratory animal care, and experiments and mouse housing were approved by the Animal
560 Welfare Committee of Université catholique de Louvain (Permit Number: 2013/UCL/MD/11
561 and 2017/UCL/MD/008). The day of vaginal plug was considered to be embryonic day (e)
562 0.5. A minimum of three embryos of the same genotype was analyzed in each experiment.
563 The embryos were collected at e12.5 and e14.5. The *Hnf6;Oc2* and the *Pou2f2* mutant mice
564 were previously described (Clotman et al. 2005, Corcoran et al. 1993, Jacquemin et al. 2000).
565 The mice and the embryos were genotyped by PCR (primer information available on
566 request).

567

568 ***In situ* hybridization (ISH) and immunofluorescence labelings**

569 For ISH, the collected embryos were fixed in ice-cold 4% paraformaldehyde (PFA) in
570 phosphate buffered-saline (PBS) overnight at 4°C, washed thrice in PBS for 10 minutes,
571 incubated in PBS/30% sucrose solution overnight at 4°C, embedded and frozen in PBS/15%
572 sucrose/7.5% gelatin. Fourteen µm section were prepared and ISH was performed as
573 previously described (Beguin et al. 2013, Francius et al. 2016, Pelosi et al. 2014) with DIG-
574 conjugated Pou2f2 (NM_011138.1, nucleotides 604-1187) or Pou2f2 exon 5b
575 (XM_006539651.3, nucleotides 643-876) antisense RNA probes.

576 For immunofluorescence, collected embryos were fixed in 4% PFA/PBS for 25 or 35 minutes
577 according to their embryonic stage and processed as for ISH. Immunolabeling was
578 performed on 14 µm serial cryosections as previously described (Francius and Clotman
579 2010). Primary antibodies against the following proteins were used: Chx10 (sheep; 1:500;
580 Exalpha Biologicals #X1179P), Foxp1 (goat; 1:1000; R&D Systems #AF4534), Gata3 (rat; 1:50;
581 Absea Biotechnology #111214D02), GFP (chick; 1:1000; Aves Lab #GFP-1020), HNF6 (guinea
582 pig; 1:2000; (Espana and Clotman 2012b); or rabbit; 1:100; Santa Cruz #sc-13050; or sheep;
583 1:1000 R&D Systems #AF6277), cMaf (rabbit; 1:3000; kindly provided by H. Wende), MafA
584 (guinea pig; 1:500; kindly provide by T. Müller), OC2 (rat; 1:400; (Clotman et al. 2005); or

585 sheep; 1:500; R&D Systems #AF6294), OC3 (guinea pig; 1:6000; (Pierreux et al. 2004)),
586 Pou2f2 (rabbit; 1:2000; Abcam #ab178679), Shox2 (mouse; 1:500; Abcam #ab55740), Sox1
587 (goat; 1:500; Santa Cruz #sc-17318). Secondary antibodies donkey anti-guinea
588 pig/AlexaFluor 488, 594 or 647, anti-mouse/AlexaFluor 488, 594 or 647, anti-
589 rabbit/AlexaFluor 594 or 647, anti-goat/AlexaFluor 488, anti-rat/AlexaFluor 647, anti-
590 sheep/AlexaFluor 594 or 647, and goat anti-mouse IgG2A specific/AlexiaFluor 488,
591 purchased from ThermoFisher Scientific or Jackson Laboratories were used at dilution
592 1:2000 or 1:1000, respectively.
593
594 ***In ovo* electroporation**
595 *In ovo* electroporations were performed at stage HH14-16, as previously described (Roy et
596 al. 2012). The coding sequence of the S_Pou2f2.4 transcript was amplified by overlapping-
597 PCR using: forward 5' GCTCTGTCTGCCCAAGAGAAA 3' and reverse 5'
598 GTTGGGACAAGGTGAGCTGT 3' primers for the 5' sequence, forward 5'
599 CCACCATCACAGCCTACCAG 3' and reverse 5' ATTATCTCGAGCCAGCCTCCTTACCCTCTCT 3'
600 (designed to enable integration at the *Xho*I restriction site of the pCMV-MCS vector) primers
601 for the 3' sequence. This sequence was first subcloned in a pCR®II-Topo® vector (Life
602 Technologies, 45-0640) for sequencing then subcloned at the *Eco*RI (from the pCR®II-Topo®
603 vector) and *Xho*I restriction sites of a pCMV-MCS vector for the *in ovo* electroporation. The
604 pCMV-Pou2f2 (0.5 μg/μl) vector was co-electroporated with a pCMV-eGFP plasmid
605 (0.25μg/μl) to visualize electroporated cells. The embryos were collected 72 hours (HH27-
606 28) after electroporation, fixed in PBS/4%PFA for 45 minutes and processed for
607 immunofluorescence labelings as previously described (Francius and Clotman 2010).
608
609 **Imaging and quantitative analyses**
610 Immunofluorescence and ISH images of cryosections were acquired on an EVOS FL Auto
611 Imaging System (Thermo Fisher Scientific) or a Confocal laser Scanning biological microscope
612 FV1000 Fluoview with the FV10-ASW 01.02 software (Olympus). The images were processed
613 with Adobe Photoshop CS5 software to match brightness and contrast with the observation.
614 Quantifications were performed on red or green or blue layer of acquired confocal images
615 and double or triple labeled cells were processed by subtractive method (Francius and
616 Clotman 2010). For each embryo ($n \geq 3$), one side of three to five sections at brachial,

617 thoracic or lumbar level were quantified using the count analysis tool of Adobe Photoshop
618 CS5 software. Raw data were exported from Adobe Photoshop CS5 software to Sigma
619 Plotv12.3 software to perform statistical analyses. The histograms were drawn with
620 Microsoft Excel. Adequate statistical tests were applied based on the number of
621 comparisons and on the variance in each group. For analysis of cell quantifications based on
622 comparison of two groups (control or mutant), standard Student's *t*-tests or Mann-Whitney
623 U tests were performed. Quantitative analyses were considered significant at $p \leq 0.05$ (Three
624 asterisks (***) indicate $p \leq 0.001$).
625 Quantitative analyzes of interneuron spatial distribution were performed as previously
626 described (Kabayiza et al. 2017). Statistical analyses of ventral IN distribution were
627 performed using a two-sample Hotelling's T2, which is a two-dimensional generalization of
628 the Student's t test. The analysis was implemented using the NCSS software package.
629
630 **Microarray analyses**
631 RNA was extracted from control or *Hnf6/Oc2* double-mutant spinal cords. The tissue was
632 manually dissociated in Tripur isolation reagent (Roche, 11 667 165 001). After dissociation,
633 chloroform (Merck Millipore, 1 02445 1000) was added to the sample, incubated at room
634 temperature for 10 minutes and centrifugated for 10 minutes at 4°C. The aqueous phase
635 was collected and the RNA was precipitated with isopropanol (VWR, 20880.310) and
636 centrifugated for 15 minutes at 4°C. The pellet was washed in ethanol (Biosolve, 06250502)
637 and centrifugated for 10 minutes at 4°C. The dried pellet was resuspended in RNAse free
638 water. The integrity of the RNA was assessed using an Agilent RNA 6000 Nano assay
639 procedure. For microarray analyzes, the RNA was converted in single-strand cDNA, labeled
640 using the GeneChip® WT PLUS Reagent Kit (Affymetrix) and hybridized on the GeneChip®
641 MoGene 2.0 ST array (Affymetrix, 90 2118) using Affymetrix devices: Genechip ® Fluidics
642 Station 450, Genechip® Hybridization oven 640, Affymetrix Genechip® scanner and the
643 Expression Consol software. The analyzes were performed using the R software. Microarray
644 data have been deposited in the GEO repository (accession number: GSE117871).
645
646 **Amplification of *Pou2f2* isoforms and sequencing**
647 Fragments of the different *Pou2f2* isoforms were amplified by RT-PCR from RNA of control B
648 lymphocytes or embryonic spinal cords purified as described above. cDNA was obtained

649 from 500 ng of RNA using the iScript™ Reverse transcriptase and the 5x iScript™ reaction
650 mix (BioRad). Conserved or divergent sequences of *Pou2f2* isoforms were amplified as
651 shown in Table 2 using a GoTaq® Green master mix (Promega, M712) or a Q5® Hot Start
652 High-Fidelity DNA Polymerase (New England BioLabs® Inc, M0493S) (primer information
653 available on request). Sequencing of the spinal *Pou2f2* exons was outsourced to Genewiz.
654 For quantitative RT-PCR, RNA was extracted from control (n = 5) or Hnf6/Oc2 double-mutant
655 (n = 4) spinal cords and purified and retrotranscribed as described above. Quantitative real-
656 time PCR was performed on 1/100 of the retrotranscription reaction using iTaq™ universal
657 SYBR® Green Supermix (BioRad, 172-5124) on a CFX Connect™ Real-Time System (BioRad)
658 with the BioRad CFX Manage 3.1 software. Each reaction was performed in duplicate and
659 relative mRNA quantities were normalized to the housekeeping gene RPL32. The B cell
660 Pou2f2 isoforms were amplified using the following primers : forward 5'
661 TGGTTCATTCCAGCATGGGG 3', reverse 5' TCCAGACTTTGCTTCTCGGC 3' and the spinal
662 Pou2f2 isoforms using : forward 5' CCACCATCACAGCCTACCAG 3', reverse 5'
663 GAGCTGGAGGAGTTGCTGTA 3' and RPL32 using: forward 5' GGCACCAGTCAGACCGATAT 3',
664 reverse 5' CAGGATCTGGCCCTTGAAC 3'. Relative expression changes between conditions
665 were calculated using the ΔΔCt method. All changes are shown as fold changes.
666

Acknowledgements

We thank members of the NEDI lab for material, technical support and discussions. We are grateful to Drs. T. Müller and H. Wende for kindly providing the guinea pig anti MafA and the rabbit anti cMaf antibodies, respectively, to Drs. F. Lemaigre and P. Jacquemin for the Hnf6/Oc2 double mutant mice, to Dr. C. Pierreux for the pCMV-MCS, to Dr. J. Ambroise for assistance with the microarray analyses and to Dr. L. Dumoutier for cDNAs of B lymphocytes. Work in the F.C. laboratory was supported by grants from the "Fonds spéciaux de recherche" (FSR) of the Université catholique de Louvain, by a "Projet de recherche (PDR)" #T.0117.13 and an "Equipement (EQP)" funding #U.N027.14 of the Fonds de la Recherche Scientifique (F.R.S.-FNRS, Belgium), by the "Actions de Recherche Concertées (ARC)" #10/15-026 of the "Direction générale de l'Enseignement non obligatoire et de la Recherche scientifique – Direction de la Recherche scientifique – Communauté française de Belgique" and granted by the "Académie universitaire 'Louvain'" and by the Association Belge contre les Maladies neuro-Musculaires. L.M.C. acknowledges funding from the Australian Government (NHMRC IRIIS and research grants #637306 and #575500) and Victorian State Government Operational Infrastructure Support. S.D. and C.B. hold PhD grants from the Fonds pour la Recherche dans l'Industrie et l'Agriculture (F.R.S.-FNRS, Belgium), M.H.-F. was a Postdoctoral Researcher of the F.R.S.-FNRS, F.C. is a Senior Research Associate of the F.R.S.-FNRS.

Competing interests: the authors declare no competing interest

689 **References**

690 Ampatzis, K., J. Song, J. Ausborn, and A. El Manira. 2014. "Separate microcircuit modules of
691 distinct v2a interneurons and motoneurons control the speed of locomotion."
692 *Neuron* 83 (4):934-43. doi: 10.1016/j.neuron.2014.07.018.
693 Audouard, E., O. Schakman, A. Ginion, L. Bertrand, P. Gailly, and F. Clotman. 2013. "The
694 Onecut transcription factor HNF-6 contributes to proper reorganization of Purkinje
695 cells during postnatal cerebellum development." *Mol Cell Neurosci* 56:159-68. doi:
696 10.1016/j.mcn.2013.05.001.
697 Audouard, E., O. Schakman, F. Rene, R. E. Huettl, A. B. Huber, J. P. Loeffler, P. Gailly, and F.
698 Clotman. 2012. "The Onecut transcription factor HNF-6 regulates in motor neurons
699 the formation of the neuromuscular junctions." *PLoS One* 7 (12):e50509. doi:
700 10.1371/journal.pone.0050509 PONE-D-12-19632 [pii].
701 Azim, E., J. Jiang, B. Alstermark, and T. M. Jessell. 2014. "Skilled reaching relies on a V2a
702 propriospinal internal copy circuit." *Nature* 508 (7496):357-63. doi:
703 10.1038/nature13021.
704 Barber, M., and A. Pierani. 2016. "Tangential migration of glutamatergic neurons and cortical
705 patterning during development: Lessons from Cajal-Retzius cells." *Dev Neurobiol* 76
706 (8):847-81. doi: 10.1002/dneu.22363.
707 Beaudry, J. B., C. E. Pierreux, G. P. Hayhurst, N. Plumb-Rudewiez, M. C. Weiss, G. G.
708 Rousseau, and F. P. Lemaigre. 2006. "Threshold levels of hepatocyte nuclear factor 6
709 (HNF-6) acting in synergy with HNF-4 and PGC-1alpha are required for time-specific
710 gene expression during liver development." *Mol Cell Biol* 26 (16):6037-46. doi:
711 26/16/6037 [pii] 10.1128/MCB.02445-05.
712 Beguin, S., V. Crepel, L. Aniksztejn, H. Becq, B. Pelosi, E. Pallesi-Pocachard, L. Bouamrane, M.
713 Pasqualetti, K. Kitamura, C. Cardoso, and A. Represa. 2013. "An epilepsy-related ARX
714 polyalanine expansion modifies glutamatergic neurons excitability and morphology
715 without affecting GABAergic neurons development." *Cereb Cortex* 23 (6):1484-94.
716 doi: 10.1093/cercor/bhs138.
717 Bikoff, J. B., M. I. Gabitto, A. F. Rivard, E. Drobac, T. A. Machado, A. Miri, S. Brenner-Morton,
718 E. Famojure, C. Diaz, F. J. Alvarez, G. Z. Mentis, and T. M. Jessell. 2016. "Spinal
719 Inhibitory Interneuron Diversity Delineates Variant Motor Microcircuits." *Cell* 165
720 (1):207-19. doi: 10.1016/j.cell.2016.01.027.
721 Blacklaws, J., D. Deska-Gauthier, C. T. Jones, Y. L. Petracca, M. Liu, H. Zhang, J. P. Fawcett, J.
722 C. Glover, G. M. Lanuza, and Y. Zhang. 2015. "Sim1 is required for the migration and
723 axonal projections of V3 interneurons in the developing mouse spinal cord." *Dev*
724 *Neurobiol* 75 (9):1003-17. doi: 10.1002/dneu.22266.
725 Boije, H., and K. Kullander. 2018. "Origin and circuitry of spinal locomotor interneurons
726 generating different speeds." *Curr Opin Neurobiol* 53:16-21. doi:
727 10.1016/j.conb.2018.04.024.
728 Borowska, J., C. T. Jones, D. Deska-Gauthier, and Y. Zhang. 2015. "V3 interneuron
729 subpopulations in the mouse spinal cord undergo distinctive postnatal maturation
730 processes." *Neuroscience* 295:221-8. doi: 10.1016/j.neuroscience.2015.03.024.
731 Borowska, J., C. T. Jones, H. Zhang, J. Blacklaws, M. Goulding, and Y. Zhang. 2013.
732 "Functional subpopulations of V3 interneurons in the mature mouse spinal cord." *J*
733 *Neurosci* 33 (47):18553-65. doi: 10.1523/JNEUROSCI.2005-13.2013.

734 Britz, O., J. Zhang, K. S. Grossmann, J. Dyck, J. C. Kim, S. Dymecki, S. Gosgnach, and M.
735 Goulding. 2015. "A genetically defined asymmetry underlies the inhibitory control of
736 flexor-extensor locomotor movements." *Elife* 4. doi: 10.7554/eLife.04718.
737 Camos, S., C. Gubern, M. Sobrado, R. Rodriguez, V. G. Romera, M. A. Moro, I. Lizasoain, J.
738 Serena, J. Mallolas, and M. Castellanos. 2014. "Oct-2 transcription factor binding
739 activity and expression up-regulation in rat cerebral ischaemia is associated with a
740 diminution of neuronal damage in vitro." *Neuromolecular Med* 16 (2):332-49. doi:
741 10.1007/s12017-013-8279-1.
742 Catela, C., M. M. Shin, and J. S. Dasen. 2015. "Assembly and function of spinal circuits for
743 motor control." *Annu Rev Cell Dev Biol* 31:669-98. doi: 10.1146/annurev-cellbio-
744 100814-125155.
745 Clotman, F., P. Jacquemin, N. Plumb-Rudewiez, C. E. Pierreux, P. Van der Smissen, H. C. Dietz,
746 P. J. Courtoy, G. G. Rousseau, and F. P. Lemaigre. 2005. "Control of liver cell fate
747 decision by a gradient of TGF beta signaling modulated by Onecut transcription
748 factors." *Genes Dev* 19 (16):1849-54. doi: 10.1101/gad.340305.
749 Clovis, Y. M., S. Y. Seo, J. S. Kwon, J. C. Rhee, S. Yeo, J. W. Lee, S. Lee, and S. K. Lee. 2016.
750 "Chx10 Consolidates V2a Interneuron Identity through Two Distinct Gene Repression
751 Modes." *Cell Rep* 16 (6):1642-52. doi: 10.1016/j.celrep.2016.06.100.
752 Corcoran, L. M., M. Karvelas, G. J. Nossal, Z. S. Ye, T. Jacks, and D. Baltimore. 1993. "Oct-2,
753 although not required for early B-cell development, is critical for later B-cell
754 maturation and for postnatal survival." *Genes Dev* 7 (4):570-82.
755 Corcoran, L. M., F. Koentgen, W. Dietrich, M. Veale, and P. O. Humbert. 2004. "All known in
756 vivo functions of the Oct-2 transcription factor require the C-terminal protein
757 domain." *J Immunol* 172 (5):2962-9.
758 Crone, S. A., K. A. Quinlan, L. Zagoraiou, S. Droho, C. E. Restrepo, L. Lundfald, T. Endo, J.
759 Setlak, T. M. Jessell, O. Kiehn, and K. Sharma. 2008. "Genetic ablation of V2a
760 ipsilateral interneurons disrupts left-right locomotor coordination in mammalian
761 spinal cord." *Neuron* 60 (1):70-83. doi: S0896-6273(08)00677-6 [pii]
762 10.1016/j.neuron.2008.08.009.
763 Dasen, J. S. 2017. "Master or servant? emerging roles for motor neuron subtypes in the
764 construction and evolution of locomotor circuits." *Curr Opin Neurobiol* 42:25-32. doi:
765 10.1016/j.conb.2016.11.005.
766 Del Barrio, M. G., R. Taveira-Marques, Y. Muroyama, D. I. Yuk, S. Li, M. Wines-Samuelson, J.
767 Shen, H. K. Smith, M. Xiang, D. Rowitch, and W. D. Richardson. 2007. "A regulatory
768 network involving Foxn4, Mash1 and delta-like 4/Notch1 generates V2a and V2b
769 spinal interneurons from a common progenitor pool." *Development* 134 (19):3427-
770 36. doi: dev.005868 [pii] 10.1242/dev.005868.
771 Dougherty, K. J., and O. Kiehn. 2010. "Firing and cellular properties of V2a interneurons in
772 the rodent spinal cord." *J Neurosci* 30 (1):24-37. doi: 10.1523/JNEUROSCI.4821-
773 09.2010.
774 Dougherty, K. J., L. Zagoraiou, D. Satoh, I. Rozani, S. Doobar, S. Arber, T. M. Jessell, and O.
775 Kiehn. 2013. "Locomotor rhythm generation linked to the output of spinal shox2
776 excitatory interneurons." *Neuron* 80 (4):920-33. doi: 10.1016/j.neuron.2013.08.015.
777 Espana, A., and F. Clotman. 2012a. "Onecut factors control development of the Locus
778 Coeruleus and of the mesencephalic trigeminal nucleus." *Mol Cell Neurosci* 50 (1):93-
779 102. doi: 10.1016/j.mcn.2012.04.002.

780 Espana, A., and F. Clotman. 2012b. "Onecut transcription factors are required for the second
781 phase of development of the A13 dopaminergic nucleus in the mouse." *J Comp*
782 *Neurol* 520 (7):1424-41. doi: 10.1002/cne.22803.
783 Francius, C., and F. Clotman. 2010. "Dynamic expression of the Onecut transcription factors
784 HNF-6, OC-2 and OC-3 during spinal motor neuron development." *Neuroscience* 165
785 (1):116-29. doi: 10.1016/j.neuroscience.2009.09.076.
786 Francius, C., and F. Clotman. 2014. "Generating spinal motor neuron diversity: a long quest
787 for neuronal identity." *Cell Mol Life Sci* 71 (5):813-29. doi: 10.1007/s00018-013-
788 1398-x.
789 Francius, C., A. Harris, V. Rucchin, T. J. Hendricks, F. J. Stam, M. Barber, D. Kurek, F. G.
790 Grosveld, A. Pierani, M. Goulding, and F. Clotman. 2013. "Identification of multiple
791 subsets of ventral interneurons and differential distribution along the rostrocaudal
792 axis of the developing spinal cord." *PLoS One* 8 (8):e70325. doi:
793 10.1371/journal.pone.0070325.
794 Francius, C., M. Hidalgo-Figueroa, S. Debrulle, B. Pelosi, V. Rucchin, K. Ronellenfitch, E.
795 Panayiotou, N. Makrides, K. Misra, A. Harris, H. Hassani, O. Schakman, C. Parras, M.
796 Xiang, S. Malas, R. L. Chow, and F. Clotman. 2016. "Vsx1 Transiently Defines an Early
797 Intermediate V2 Interneuron Precursor Compartment in the Mouse Developing
798 Spinal Cord." *Front Mol Neurosci* 9:145. doi: 10.3389/fnmol.2016.00145.
799 Goetz, C., C. Pivetta, and S. Arber. 2015. "Distinct limb and trunk premotor circuits establish
800 laterality in the spinal cord." *Neuron* 85 (1):131-144. doi:
801 10.1016/j.neuron.2014.11.024.
802 Gosgnach, S., J. B. Bikoff, K. J. Dougherty, A. El Manira, G. M. Lanuza, and Y. Zhang. 2017.
803 "Delineating the Diversity of Spinal Interneurons in Locomotor Circuits." *J Neurosci*
804 37 (45):10835-10841. doi: 10.1523/JNEUROSCI.1829-17.2017.
805 Grossmann, K. S., A. Giraudin, O. Britz, J. Zhang, and M. Goulding. 2010. "Genetic dissection
806 of rhythmic motor networks in mice." *Prog Brain Res* 187:19-37. doi: 10.1016/B978-
807 0-444-53613-6.00002-2.
808 Guo, J., and E. S. Anton. 2014. "Decision making during interneuron migration in the
809 developing cerebral cortex." *Trends Cell Biol* 24 (6):342-51. doi:
810 10.1016/j.tcb.2013.12.001.
811 Hatzopoulos, A. K., A. S. Stoykova, J. R. Erselius, M. Goulding, T. Neuman, and P. Gruss. 1990.
812 "Structure and expression of the mouse Oct2a and Oct2b, two differentially spliced
813 products of the same gene." *Development* 109 (2):349-62.
814 Hayashi, M., C. A. Hinckley, S. P. Driscoll, N. J. Moore, A. J. Levine, K. L. Hilde, K. Sharma, and
815 S. L. Pfaff. 2018. "Graded Arrays of Spinal and Supraspinal V2a Interneuron Subtypes
816 Underlie Forelimb and Hindlimb Motor Control." *Neuron* 97 (4):869-884 e5. doi:
817 10.1016/j.neuron.2018.01.023.
818 Hilde, K. L., A. J. Levine, C. A. Hinckley, M. Hayashi, J. M. Montgomery, M. Gullo, S. P. Driscoll,
819 R. Grosschedl, Y. Kohwi, T. Kohwi-Shigematsu, and S. L. Pfaff. 2016. "Satb2 Is
820 Required for the Development of a Spinal Exteroceptive Microcircuit that Modulates
821 Limb Position." *Neuron* 91 (4):763-776. doi: 10.1016/j.neuron.2016.07.014.
822 Hodson, D. J., A. L. Shaffer, W. Xiao, G. W. Wright, R. Schmitz, J. D. Phelan, Y. Yang, D. E.
823 Webster, L. Rui, H. Kohlhammer, M. Nakagawa, T. A. Waldmann, and L. M. Staudt.
824 2016. "Regulation of normal B-cell differentiation and malignant B-cell survival by
825 OCT2." *Proc Natl Acad Sci U S A* 113 (14):E2039-46. doi: 10.1073/pnas.1600557113.

826 Jacquemin, P., S. M. Durviaux, J. Jensen, C. Godfraind, G. Gradwohl, F. Guillemot, O. D.
827 Madsen, P. Carmeliet, M. Dewerchin, D. Collen, G. G. Rousseau, and F. P. Lemaigre.
828 2000. "Transcription factor hepatocyte nuclear factor 6 regulates pancreatic
829 endocrine cell differentiation and controls expression of the proendocrine gene
830 ngn3." *Mol Cell Biol* 20 (12):4445-54.
831 Jacquemin, P., V. J. Lannoy, G. G. Rousseau, and F. P. Lemaigre. 1999. "OC-2, a novel
832 mammalian member of the ONECUT class of homeodomain transcription factors
833 whose function in liver partially overlaps with that of hepatocyte nuclear factor-6." *J*
834 *Biol Chem* 274 (5):2665-71.
835 Jacquemin, P., F. P. Lemaigre, and G. G. Rousseau. 2003. "The Onecut transcription factor
836 HNF-6 (OC-1) is required for timely specification of the pancreas and acts upstream
837 of Pdx-1 in the specification cascade." *Dev Biol* 258 (1):105-16. doi:
838 S0012160603001155 [pii].
839 Jacquemin, P., C. E. Pierreux, S. Fierens, J. M. van Eyll, F. P. Lemaigre, and G. G. Rousseau.
840 2003. "Cloning and embryonic expression pattern of the mouse Onecut transcription
841 factor OC-2." *Gene Expr Patterns* 3 (5):639-44. doi: S1567133X03001108 [pii].
842 Joshi, K., S. Lee, B. Lee, J. W. Lee, and S. K. Lee. 2009. "LMO4 controls the balance between
843 excitatory and inhibitory spinal V2 interneurons." *Neuron* 61 (6):839-51. doi:
844 10.1016/j.neuron.2009.02.011.
845 Kabayiza, K. U., G. Masgutova, A. Harris, V. Rucchin, B. Jacob, and F. Clotman. 2017. "The
846 Onecut Transcription Factors Regulate Differentiation and Distribution of Dorsal
847 Interneurons during Spinal Cord Development." *Front Mol Neurosci* 10:157. doi:
848 10.3389/fnmol.2017.00157.
849 Konig, H., P. Pfisterer, L. M. Corcoran, and T. Wirth. 1995. "Identification of CD36 as the first
850 gene dependent on the B-cell differentiation factor Oct-2." *Genes Dev* 9 (13):1598-
851 607.
852 Lai, H. C., R. P. Seal, and J. E. Johnson. 2016. "Making sense out of spinal cord somatosensory
853 development." *Development* 143 (19):3434-3448. doi: 10.1242/dev.139592.
854 Landry, C., F. Clotman, T. Hioki, H. Oda, J. J. Picard, F. P. Lemaigre, and G. G. Rousseau. 1997.
855 "HNF-6 is expressed in endoderm derivatives and nervous system of the mouse
856 embryo and participates to the cross-regulatory network of liver-enriched
857 transcription factors." *Dev Biol* 192 (2):247-57. doi: 10.1006/dbio.1997.8757.
858 Lannoy, V. J., A. Rodolosse, C. E. Pierreux, G. G. Rousseau, and F. P. Lemaigre. 2000.
859 "Transcriptional stimulation by hepatocyte nuclear factor-6. Target-specific
860 recruitment of either CREB-binding protein (CBP) or p300/CBP-associated factor
861 (p/CAF)." *J Biol Chem* 275 (29):22098-103. doi: 10.1074/jbc.M000855200
862 M000855200 [pii].
863 Latchman, D. S. 1996. "The Oct-2 transcription factor." *Int J Biochem Cell Biol* 28 (10):1081-
864 3.
865 Lee, S., B. Lee, K. Joshi, S. L. Pfaff, J. W. Lee, and S. K. Lee. 2008. "A regulatory network to
866 segregate the identity of neuronal subtypes." *Dev Cell* 14 (6):877-89. doi: S1534-
867 5807(08)00132-9 [pii] 10.1016/j.devcel.2008.03.021.
868 Lemaigre, F. P., S. M. Durviaux, O. Truong, V. J. Lannoy, J. J. Hsuan, and G. G. Rousseau. 1996.
869 "Hepatocyte nuclear factor 6, a transcription factor that contains a novel type of
870 homeodomain and a single cut domain." *Proc Natl Acad Sci U S A* 93 (18):9460-4.
871 Lillycrop, K. A., and D. S. Latchman. 1992. "Alternative splicing of the Oct-2 transcription
872 factor RNA is differentially regulated in neuronal cells and B cells and results in

protein isoforms with opposite effects on the activity of octamer/TAATGARAT-containing promoters." *J Biol Chem* 267 (35):24960-5.

Liu, Y. Z., K. A. Lillycrop, and D. S. Latchman. 1995. "Regulated splicing of the Oct-2 transcription factor RNA in neuronal cells." *Neurosci Lett* 183 (1-2):8-12.

Lu, D. C., T. Niu, and W. A. Alaynick. 2015. "Molecular and cellular development of spinal cord locomotor circuitry." *Front Mol Neurosci* 8:25. doi: 10.3389/fnmol.2015.00025.

Misra, K., H. Luo, S. Li, M. Matise, and M. Xiang. 2014. "Asymmetric activation of Dll4-Notch signaling by Foxn4 and proneural factors activates BMP/TGFbeta signaling to specify V2b interneurons in the spinal cord." *Development* 141 (1):187-98. doi: 10.1242/dev.092536.

Panayi, H., E. Panayiotou, M. Orford, N. Genethliou, R. Mean, G. Lapathitis, S. Li, M. Xiang, N. Kessaris, W. D. Richardson, and S. Malas. 2010. "Sox1 is required for the specification of a novel p2-derived interneuron subtype in the mouse ventral spinal cord." *J Neurosci* 30 (37):12274-80. doi: 10.1523/JNEUROSCI.2402-10.2010.

Pelosi, B., S. Migliarini, G. Pacini, M. Pratelli, and M. Pasqualetti. 2014. "Generation of Pet1210-Cre transgenic mouse line reveals non-serotonergic expression domains of Pet1 both in CNS and periphery." *PLoS One* 9 (8):e104318. doi: 10.1371/journal.pone.0104318.

Peng, C. Y., H. Yajima, C. E. Burns, L. I. Zon, S. S. Sisodia, S. L. Pfaff, and K. Sharma. 2007. "Notch and MAML signaling drives Scl-dependent interneuron diversity in the spinal cord." *Neuron* 53 (6):813-27. doi: S0896-6273(07)00139-0 [pii] 10.1016/j.neuron.2007.02.019.

Pierreux, C. E., V. Vanhorenbeeck, P. Jacquemin, F. P. Lemaigre, and G. G. Rousseau. 2004. "The transcription factor hepatocyte nuclear factor-6/Onecut-1 controls the expression of its paralog Onecut-3 in developing mouse endoderm." *J Biol Chem* 279 (49):51298-304. doi: 10.1074/jbc.M409038200 M409038200 [pii].

Pivetta, C., M. S. Esposito, M. Sigrist, and S. Arber. 2014. "Motor-circuit communication matrix from spinal cord to brainstem neurons revealed by developmental origin." *Cell* 156 (3):537-48. doi: 10.1016/j.cell.2013.12.014.

Roy, A., C. Francius, D. L. Rousso, E. Seuntjens, J. Debruyn, G. Luxenhofer, A. B. Huber, D. Huylebroeck, B. G. Novitch, and F. Clotman. 2012. "Onecut transcription factors act upstream of Isl1 to regulate spinal motoneuron diversification." *Development* 139 (17):3109-19. doi: 10.1242/dev.078501.

Stam, F. J., T. J. Hendricks, J. Zhang, E. J. Geiman, C. Francius, P. A. Labosky, F. Clotman, and M. Goulding. 2012. "Renshaw cell interneuron specialization is controlled by a temporally restricted transcription factor program." *Development* 139 (1):179-90. doi: 10.1242/dev.071134.

Stoykova, A. S., S. Sterrer, J. R. Erselius, A. K. Hatzopoulos, and P. Gruss. 1992. "Mini-Oct and Oct-2c: two novel, functionally diverse murine Oct-2 gene products are differentially expressed in the CNS." *Neuron* 8 (3):541-58.

Surmeli, G., T. Akay, G. C. Ippolito, P. W. Tucker, and T. M. Jessell. 2011. "Patterns of spinal sensory-motor connectivity prescribed by a dorsoventral positional template." *Cell* 147 (3):653-65. doi: S0092-8674(11)01210-4 [pii] 10.1016/j.cell.2011.10.012.

Sweeney, L. B., J. B. Bikoff, M. I. Gabitto, S. Brenner-Morton, M. Baek, J. H. Yang, E. G. Tabak, J. S. Dasen, C. R. Kintner, and T. M. Jessell. 2018. "Origin and Segmental Diversity of Spinal Inhibitory Interneurons." *Neuron* 97 (2):341-355 e3. doi: 10.1016/j.neuron.2017.12.029.

920 Talpalar, A. E., J. Bouvier, L. Borgius, G. Fortin, A. Pierani, and O. Kiehn. 2013. "Dual-mode
921 operation of neuronal networks involved in left-right alternation." *Nature* 500
922 (7460):85-8. doi: 10.1038/nature12286.
923 Thaler, J. P., S. K. Lee, L. W. Jurata, G. N. Gill, and S. L. Pfaff. 2002. "LIM factor Lhx3
924 contributes to the specification of motor neuron and interneuron identity through
925 cell-type-specific protein-protein interactions." *Cell* 110 (2):237-49. doi:
926 S0092867402008231 [pii].
927 Theodorou, E., G. Dalembert, C. Heffelfinger, E. White, S. Weissman, L. Corcoran, and M.
928 Snyder. 2009. "A high throughput embryonic stem cell screen identifies Oct-2 as a
929 bifunctional regulator of neuronal differentiation." *Genes Dev* 23 (5):575-88. doi:
930 10.1101/gad.1772509.
931 Tripodi, M., A. E. Stepien, and S. Arber. 2011. "Motor antagonism exposed by spatial
932 segregation and timing of neurogenesis." *Nature* 479 (7371):61-6. doi: nature10538
933 [pii] 10.1038/nature10538.
934 Vanhorenbeeck, V., P. Jacquemin, F. P. Lemaigre, and G. G. Rousseau. 2002. "OC-3, a novel
935 mammalian member of the ONECUT class of transcription factors." *Biochem Biophys*
936 *Res Commun* 292 (4):848-54. doi: 10.1006/bbrc.2002.6760 S0006291X02967604 [pii].
937 Wirth, T., A. Priess, A. Annweiler, S. Zwilling, and B. Oeler. 1991. "Multiple Oct2 isoforms are
938 generated by alternative splicing." *Nucleic Acids Res* 19 (1):43-51.
939 Ziskind-Conhaim, L., and S. Hochman. 2017. "Diversity of molecularly defined spinal
940 interneurons engaged in mammalian locomotor pattern generation." *J Neurophysiol*
941 118 (6):2956-2974. doi: 10.1152/jn.00322.2017.
942
943
944
945

946 **Figure legends**

947

948 **Figure 1.** OC factors are present in multiple subsets of V2 interneurons. **(A-I")**
949 Immunolabelings for OC, the V2a generic marker Chx10 and markers of V2a subpopulations
950 (Francius et al. 2013) on transverse spinal cord sections (brachial or thoracic levels) of e12.5
951 wild-type mouse embryos. In each figure, the right ventral quadrant of the spinal cord is
952 shown. Only HNF-6 is detected in Shox2+ V2a cells (arrow in A-C''), whereas the 3 OC are
953 present in the MafA+ and in the cMaf+ V2a subsets (arrows in D-I"). **(J-L")** Immunolabelings
954 for OC, the V2b generic marker Gata3 and MafA. The 3 OC proteins are detected in MafA+
955 V2b interneurons (arrows). **(M-O")** Immunolabelings for OC and the V2c marker Sox1
956 demonstrate that OC factors are present in a majority of V2c interneurons (arrows). Sox1 in
957 the ventricular zone labels neural progenitors. Scale bar = 50 µm.

958

959 **Figure 2.** OC factors regulate the diversification of the V2 interneurons. Immunolabelings on
960 transverse spinal cord sections (brachial or thoracic levels) of control or *Hnf6*$^{-/-}$*;Oc2*$^{-/-}$ double-
961 mutant embryos. At e12.5 **(A-C)** and e14.5 **(D)**, the production of the V2a Chx10+
962 interneurons is not altered in the absence of OC factors. Similarly, the number of
963 Shox2+ V2a is affected neither at e12.5 **(E-G)** nor at e14.5 **(H)**. In contrast, quantitative
964 analysis of control or *Hnf6*$^{-/-}$*;Oc2*$^{-/-}$ littermates at e12.5 **(I-K)** and at e14.5 **(L)** shows reduction
965 in MafA+ V2a interneurons in double mutants as compared to control embryos. Similarly,
966 the number of cMaf+ V2a interneurons is significantly reduced at e12.5 (**M-O**) and e14.5 (**P**)
967 in the absence of OC factors. At e12.5 **(Q-S)** and e14.5 **(T)**, the production of the V2b
968 interneurons is not affected in *Hnf6*$^{-/-}$*;Oc2*$^{-/-}$ embryos. The generation of the MafA+ V2b
969 interneurons is also unchanged at e12.5 **(U-W)** or e14.5 **(X)**. At e12.5 **(Y-AA)**, the number of
970 V2c interneurons is dramatically reduced in the absence of OC factors (Sox1 in the
971 ventricular zone labels neural progenitors). However, this is no longer the case at e14.5 **(BB)**.
972 Mean values ± SEM. * $p \leq 0.05$; ** $p \leq 0.01$; *** $p \leq 0.001$. Scale bar = 50 µm.

973

974 **Figure 3.** OC factors regulate the distribution of V2a interneurons. Distribution of V2a
975 interneurons on transverse section of the spinal cord in control or *Hnf6*$^{-/-}$*;Oc2*$^{-/-}$ double-
976 mutant embryos at brachial, thoracic or lumbar level (only the right hemisection is shown).
977 Two-dimension distribution graphs (left) show integration of cell distribution from multiple

978 sections of multiple embryos of each genotype. One-dimension graphs (right) compare
979 density distribution in control (blue) and in double-mutant embryos (red) on the dorso-
980 ventral (upper) or the medio-lateral (lower) axis of the spinal cord (see Materials and
981 methods for details). **(A-C)** At e12.5 in control embryos, V2a interneurons distribute in 2
982 connected clusters, a major central group and a minor medial group, at each level of the
983 spinal cord. **(D-L)** In mutant embryos, the relative cell distribution between the 2 clusters
984 seems altered, with relatively less central cells at brachial level and less medial cells at
985 lumbar levels (n=3, p≤0.001). **(M-X)** Altered V2a distribution on the mediolateral axis is
986 confirmed at e14.5. **(M-O, S-X)** In control embryos, the 2 V2a groups coalesce in a more
987 evenly-distributed population that occupied ~70% of the medio-lateral axis. **(P-X)** In mutant
988 embryos, V2a interneurons remain segregated into 2 distinct, although connected, clusters
989 with a majority of cells in medial position (n=3, p≤0.001). **(Y-VV)** Similar observations are
990 made for the Shox2+ V2a subpopulation. At e12.5 in control embryos **(Y-AA)**, Shox2+ V2a
991 distribute in a minor medial and a major lateral cluster. **(BB-JJ)** In mutant embryos, these
992 cells are slightly more ventral at brachial level and distribute more evenly between the two
993 clusters at brachial and lumbar levels (n=3, p≤0.001). **(KK-VV)** At e14.5, Shox2+ V2a in the
994 mutant were slightly more ventral and remained more medial than in control embryos (n=3,
995 p≤0.001).
996
997 **Figure 4.** OC factors regulate the distribution of V2b interneurons. **(A-C)** At e12.5 in control
998 embryos, V2b cells are distributed in a major central (brachial level) or lateral (thoracic and
999 lumbar levels) cluster with minor subsets located more medially (arrows) or ventrally
1000 (arrowheads). **(D-L)** In OC mutant embryos at e12.5, the major population remains more
1001 compact, more centrally located and slightly more ventral. In addition, the ventral V2b
1002 subset is significantly depleted (asterisks; n=3, p≤0.001). **(M-X)** Consistently, at e14.5, V2b
1003 interneurons in the central cluster are more compact in the absence of OC factors, and a
1004 small contingent of V2b migrating towards the medio-dorsal spinal cord in control embryos
1005 (arrowheads) is missing in OC mutant littermates (asterisks; n=3, p≤0.001 at brachial level;
1006 p=0.080 and 0.112 at thoracic and lumbar levels, repsectively).
1007
1008 **Figure 5.** OC factors control expression of spinal cord-specific isoforms of *Pou2f2*. **(A)** The
1009 different Pou2f2 isoforms present in the B cells (B_Pou2f2) are characterized by invariant

1010 exons (dark grey) and alternative exons 4, 5, 8, 14 or 16 (light grey). They contain a POU-
1011 specific domain (light green) encoded by exons 9 and 10 and a POU-type homeodomain
1012 (dark green) encoded by exons 11 and 12. The 4 spinal Pou2f2 isoforms (S_Pou2f2.1 to
1013 S_Pou2f2.4) (identified in the spinal cord) are characterized by a distinct exon 1 (E1X in light
1014 orange), an additional exon E5b (dark orange) and alternative exons E1b and 4 (medium
1015 orange and light grey, respectively). The presence of E1b disrupts the reading frame and
1016 imposes the use of the ATG located in E2a, whereas the absence of E1b leaves open the use
1017 of the ATG located in E1X. The regions corresponding to the generic or to the E5b *in situ*
1018 hybridization probes are indicated. **(B-E)** Quantification of spinal Pou2f2 or B-cell isoforms by
1019 RT-qPCR. **(B)** In control spinal cords, spinal Pou2f2 isoforms are >30-fold more abundant
1020 than B-cell isoforms. **(C)** B cell Pou2f2 isoforms barely trend to increase in the absence of OC
1021 factors. **(D)** In contrast, spinal Pou2f2 isoforms are 2.6-fold overexpressed in *Hnf6*$^{-/-}$;*Oc2*$^{-/-}$
1022 spinal cords. **(E)** In double mutant spinal cords, spinal Pou2f2 isoforms are >60-fold more
1023 abundant than B-cell isoforms. **(F-I)** *In situ* hybridization labelings on transverse sections
1024 (brachial level) of control or *Hnf6*$^{-/-}$;*Oc2*$^{-/-}$ spinal cords at e11.5 with **(F-G)** a generic *Pou2f2*
1025 probe complementary to spinal and to B-cell isoforms **(A)** or **(H-I)** a spinal isoform-specific
1026 probe corresponding only to exon E5b **(A)**. **(F, H)** In control embryos, *Pou2f2* is strongly
1027 expressed in ventral and in dorsal interneuron populations, and more weakly in the ventral
1028 motor neuron area. **(G, I)** In OC mutant embryos, *Pou2f2* is upregulated in interneuron
1029 populations and its expression is expanded in ventral populations (arrowheads) and in the
1030 motor neurons (arrows). * $p \leq 0.05$; ** $p \leq 0.01$. Scale bars = 50 µm.
1031
1032 **Figure 6.** The Pou2f2+ V2a interneurons are mislocated in the absence of OC factors. **(A-F)**
1033 Immunolabelings and quantification of Pou2f2+ V2a interneurons in control or *Hnf6*$^{-/-}$;*Oc2*$^{-/-}$
1034 mutant embryos. At e12.5 **(A-B)** and e14.5 **(C-D)**, Pou2f2 is detected in V2a Chx10^{+}
1035 interneurons, and the number of Pou2f2-containing Chx10+ cells trends to increase but is
1036 not significantly different in the absence of OC factors **(E-F)**. **(G-DD)** Distribution of Pou2f2+
1037 V2a interneurons on transverse section of the spinal cord in control or *Hnf6*$^{-/-}$;*Oc2*$^{-/-}$ double-
1038 mutant embryos. One-dimension graphs (lower) show density distribution on the dorso-
1039 ventral (left) or the medio-lateral (right) axis of the spinal cord. **(G-R)** At e12.5, cells in the
1040 central clusters are slightly reduced at brachial and at thoracic levels in the absence of OC
1041 factors (n=3, $p \leq 0.001$). **(S-DD)** At e14.5, a vast majority of V2a containing Pou2f2 settle in a

1042 more medial position in *Hnf6*$^{-/-}$;*Oc2*$^{-/-}$ spinal cords (n=3, p≤0.001). Mean values ± SEM. Scale
1043 bar = 50 µm.
1044
1045 **Figure 7.** The Pou2f2+ V2b interneurons are mislocated in the absence of OC factors. **(A-F)**
1046 Immunolabelings and quantification of Pou2f2+ V2b interneurons in control or *Hnf6*$^{-/-}$;*Oc2*$^{-/-}$
1047 mutant embryos. At e12.5 **(A-B)** and e14.5 **(C-D)**, Pou2f2 is present in V2b Gata3+
1048 interneurons, but the number of Pou2f2+ V2b cells was not significantly increased **(E-F)**. **(G-**
1049 **DD)** Distribution of Pou2f2+ V2b interneurons on transverse section of the spinal cord in
1050 control or *Hnf6*$^{-/-}$;*Oc2*$^{-/-}$ double-mutant embryos. One-dimension graphs (lower) show
1051 density distribution on the dorso-ventral (left) or the medio-lateral (right) axis of the spinal
1052 cord. **(G-R)** At e12.5, Pou2f2-containing V2b are more central and slightly more ventral in the
1053 absence of OC factors (n=3, p≤0.001). **(S-DD)** At e14.5, this subset of V2b interneurons is
1054 more clustered on the medio-lateral axis in *Hnf6*$^{-/-}$;*Oc2*$^{-/-}$ spinal cords (n=3, p≤0.001). Mean
1055 values ± SEM. Scale bar = 50 µm.
1056
1057 **Figure 8.** V2 interneuron distribution is altered after misexpression of *Pou2f2.*
1058 Overexpression of *Pou2f2* in chick embryonic spinal cord after electroporation at HH14-16
1059 and immunolabelings 72 hours after electroporation. **(A-B, O-P)** At HH27-28, *Pou2f2*
1060 overexpression does not impact the number of V2a (Chx10+) **(K)**, Shox2+ V2a **(L)**, V2b **(M)** or
1061 V2d **(N)** interneurons. **(C-J, Q-T)** In contrast, it alters V2 distribution. **(C-J)** In control spinal
1062 cord, V2a and Shox2+ V2a interneurons are distributed in two closely connected clusters on
1063 the medio-lateral axis of the neuroepithelium. In electroporated spinal cord, lateral
1064 migration is increased and a majority of V2a and Shox2+ V2a interneurons are clustered in a
1065 single central group with ectopic lateral extensions (arrows; n=3, p≤0.001). **(Q-T)** In control
1066 spinal cord, V2b are distributed in two groups along the medio-lateral axis with a majority of
1067 cells in the lateral cluster. In electroporated spinal cord, lateral migration of the V2b
1068 interneurons is reduced and a majority of cells is located in the medial cluster (n=3,
1069 p≤0.001). Mean values ± SEM. Scale bar = 50 µm.
1070
1071 **Figure 9.** Pou2f2 regulate the distribution of V2a interneurons. **(A-G)** Immunolabelings and
1072 quantification of V2a, Shox2+ V2a and V2d interneurons in control or *Pou2f2*$^{-/-}$ mutant
1073 embryos. **(A-B, E)** At e12.5, the production of the Chx10+ V2a interneurons is not altered in

1074 absence of Pou2f2. **(C-D, F-G)** Similarly, neither the number of Shox2+ V2a nor the number
1075 of V2d interneurons are affected in *Pou2f2*$^{-/-}$ mutants. **(H-EE)** Distribution of V2a and Shox2+
1076 V2a interneurons on transverse section of the spinal cord in control or *Pou2f2*$^{-/-}$ mutant
1077 embryos. One-dimension graphs (lower) show density distribution on the dorso-ventral (left)
1078 or the medio-lateral (right) axis of the spinal cord. **(H-S)** V2a distribution is affected in
1079 *Pou2f2*$^{-/-}$ mutants. As compared to the two V2a clusters observed in control embryos,
1080 Chx10+ cells are relatively more abundant in the medial cluster in *Pou2f2*$^{-/-}$ mutant embryos
1081 (n=3, p≤0.001). **(T-EE)** Similarly, Shox2+ V2a remained more medial at brachial level, but
1082 migrated more laterally at lumbar level (n=3, p≤0.001). Mean values ± SEM. Scale bar = 50
1083 µm.
1084
1085 **Figure 10.** Pou2f2 regulate the distribution of V2b interneurons. **(A-G)** Immunolabelings and
1086 quantification of V2b interneurons in control or *Pou2f2*$^{-/-}$ mutant embryos. At e12.5, the
1087 production of the Gata3+ V2b interneurons is not affected by the absence of Pou2f2. **(D-O)**
1088 Distribution of V2b interneurons on transverse section of the spinal cord in control or
1089 *Pou2f2*$^{-/-}$ mutant embryos. One-dimension graphs (lower) show density distribution on the
1090 dorso-ventral (left) or the medio-lateral (right) axis of the spinal cord. **(D-O)** The distribution
1091 of V2b cells is altered in *Pou2f2*$^{-/-}$ mutants, as V2b interneurons remained more medial at
1092 thoracic level but migrated more laterally at lumbar level (n=3, p≤0.001). Mean values ±
1093 SEM. Scale bar = 50 µm.
1094
1095
1096
1097 **Supporting figure legends**
1098
1099 **Supplementary Figure S1.** OC factors regulate the diversification of the V2 interneurons. **(A-**
1100 **H'')** Immunolabelings of the V2a generic marker Chx10 and markers of V2a subpopulations
1101 on transverse spinal cord sections (brachial or thoracic levels) control or *Hnf6*$^{-/-}$*;Oc2*$^{-/-}$
1102 mutant embryos at e14.5. Quantifications are shown in Fig 1. V2a **(A-B),** Shox2+ V2a (arrows)
1103 and V2d interneurons (**C- D''**, arrowheads) are present in both control and double mutant
1104 embryos. **(E-E'')** MafA is present in a V2a supbopulation in control embryos (arrows), **(F-F'')**
1105 but is not detected in Chx10+ cells in the absence of OC factors. **(G-G'')** Similarly**,** cMaf is

1106 present in a subpopulation of V2a interneurons in control embryos (arrows), **(H-H'')** which is
1107 not the case in *Hnf6*$^{-/-}$;*Oc2*$^{-/-}$ embryos. **(I-L'')** Immunolabelings of the V2b generic marker
1108 Gata3 and the marker of V2b subpopulation, MafA. V2b **(I-J'')** and MafA+ V2b (**K-L''**, arrows)
1109 interneurons are present in control and in *Hnf6*$^{-/-}$;*Oc2*$^{-/-}$ embryos. **(M-N)** The number of V2c
1110 interneurons is unchanged is similarly detected in *Hnf6*$^{-/-}$;*Oc2*$^{-/-}$ embryos as compared to
1111 control embryos (delineated cells). Sox1 in the ventricular zone labels neural progenitors.
1112 Scale bar = 50 µm.
1113
1114 **Supplementary Figure S2.** Pou2f2 RT-PCR experiments and sequence of the spinal Pou2f2
1115 exon 1b and exon 5b. Composite assembly of electrophoresis images of RT-PCR amplification
1116 products for *Pou2f2* isoform sequences on embryonic spinal cord or B-cell RNA samples.
1117 Water was used as a negative control (Ctl-). **(A)** Amplifications from exon 1 (E1) to E6 on
1118 embryonic spinal cord RNA samples (asterisk) fail to amplify the RNA isoforms detected in B
1119 cell samples. In contrast, amplifications from E7 to E9, from E10 to E12 and from E13 to E17
1120 show at least one similar amplicon in spinal cord samples and in B cell samples. **(B)**
1121 Amplification from E1 (other forward primer) to E7 also fails to amplify *Pou2f2* spinal cord
1122 isoforms. In contrast, amplifications from E2, 3, 4 and 5 to E7 produce systematically longer
1123 amplicons in spinal cord samples (arrowheads) as compared to B cell samples. The E6 to E7
1124 amplification is similar in both samples. **(C)** Amplifications from E1X (present in the X6
1125 sequence) to E3 do not produce amplicon in B-cell samples (asterisk). Amplifications from
1126 E1X to E3 or to E5b on spinal cord samples systematically produce 2 amplicons
1127 (arrowheads). Amplifications of the E5b exon sequence, from E3 to E5b and from E5b to E7
1128 produce expected amplicons in spinal cord samples. **(D)** Comparison of exon 1b and exon 5b
1129 sequences in the predicted X6 sequence and the sequenced embryonic spinal cord *Pou2f2*
1130 isoforms. Sequences of E1X, E2a and E5b exons align (100% identity) with the predicted X6
1131 sequence. Sequence of the additional alterative exon 1b is shown. SD = Size standard, E =
1132 Exon, SC = Embryonic spinal cord, B = B lymphocytes.
1133
1134 **Supplementary Figure S3.** The number of Pou2f2+Shox2+ V2a interneurons is normal in
1135 *Hnf6*$^{-/-}$;*Oc2*$^{-/-}$ mutant embryos. Immunolabelings on transverse spinal cord sections (brachial
1136 or thoracic levels) of control or *Hnf6*$^{-/-}$;*Oc2*$^{-/-}$ mutant embryos. At e12.5 **(A-C)** and at e14.5

1137 **(D-F)**, the number of V2a containing Shox2 and Pou2f2 is unchanged in the absence of OC
1138 factors. Mean values ± SEM. Scale bar = 50 µm.
1139
1140 **Supplementary Figure S4.** Efficacy of pCMV-eGFP and pCMV-Pou2f2 co-electroporation in
1141 the chicken embryonic spinal cord. **(A-C)** eGFP (green, **B**) and Pou2f2 (red, **C**) are present in a
1142 vast majority of cells along the dorso-ventral axis of the spinal cord. Scale bar = 50 µm.
1143
1144 **Supplementary Figure S5.** The number of MafA+ or cMaf+ V2a interneurons is normal in
1145 *Pou2f2*$^{-/-}$ mutant spinal cords. Immunolabelings on transverse spinal cord sections (brachial
1146 or thoracic levels) of control or *Pou2f2*$^{-/-}$ mutant embryos at e12.5. **(A-F)** Absence of Pou2f2
1147 does not impact on the number of MafA+ **(A-C)** or cMaf+ V2a interneurons **(D-F)**. Mean
1148 values ± SEM. Scale bar = 50 µm.
1149
1150 **Supplementary Figure S6.** The number of MafA-positive V2b interneurons or of the V2c
1151 interneurons is normal in *Pou2f2*$^{-/-}$ mutant spinal cords. Immunolabelings on transverse
1152 spinal cord sections (brachial or thoracic levels) of control or *Pou2f2*$^{-/-}$ mutant embryos at
1153 e12.5. **(A-B, E)** The number of MafA+ V2b interneurons is not significantly altered in the
1154 absence of Pou2f2. **(C-D, F)** Similarly, the production of V2c interneurons is not affected in
1155 *Pou2f2* mutants. Mean values ± SEM. Scale bar = 50 µm.
1156

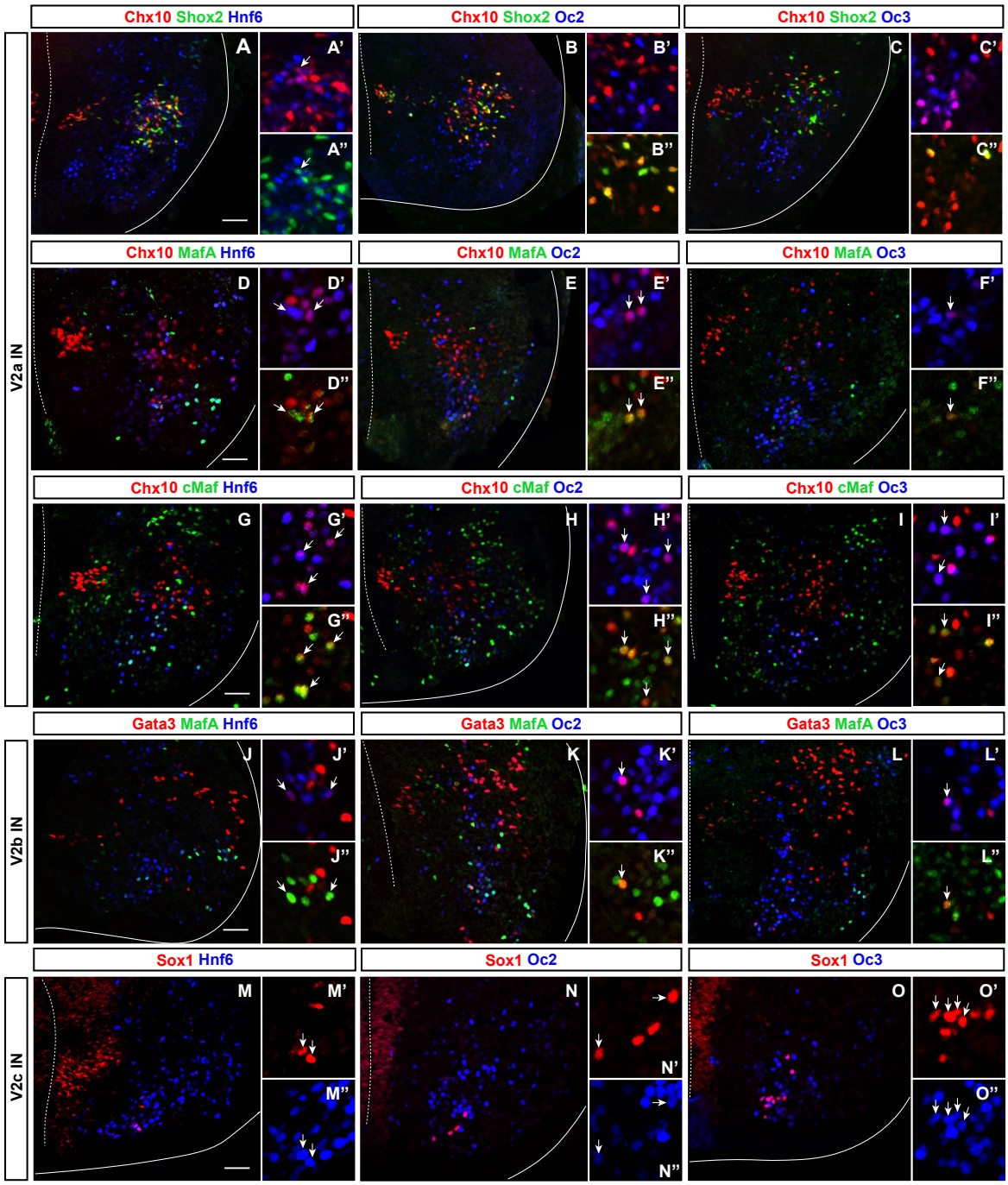

Harris A. et al, Figure 1

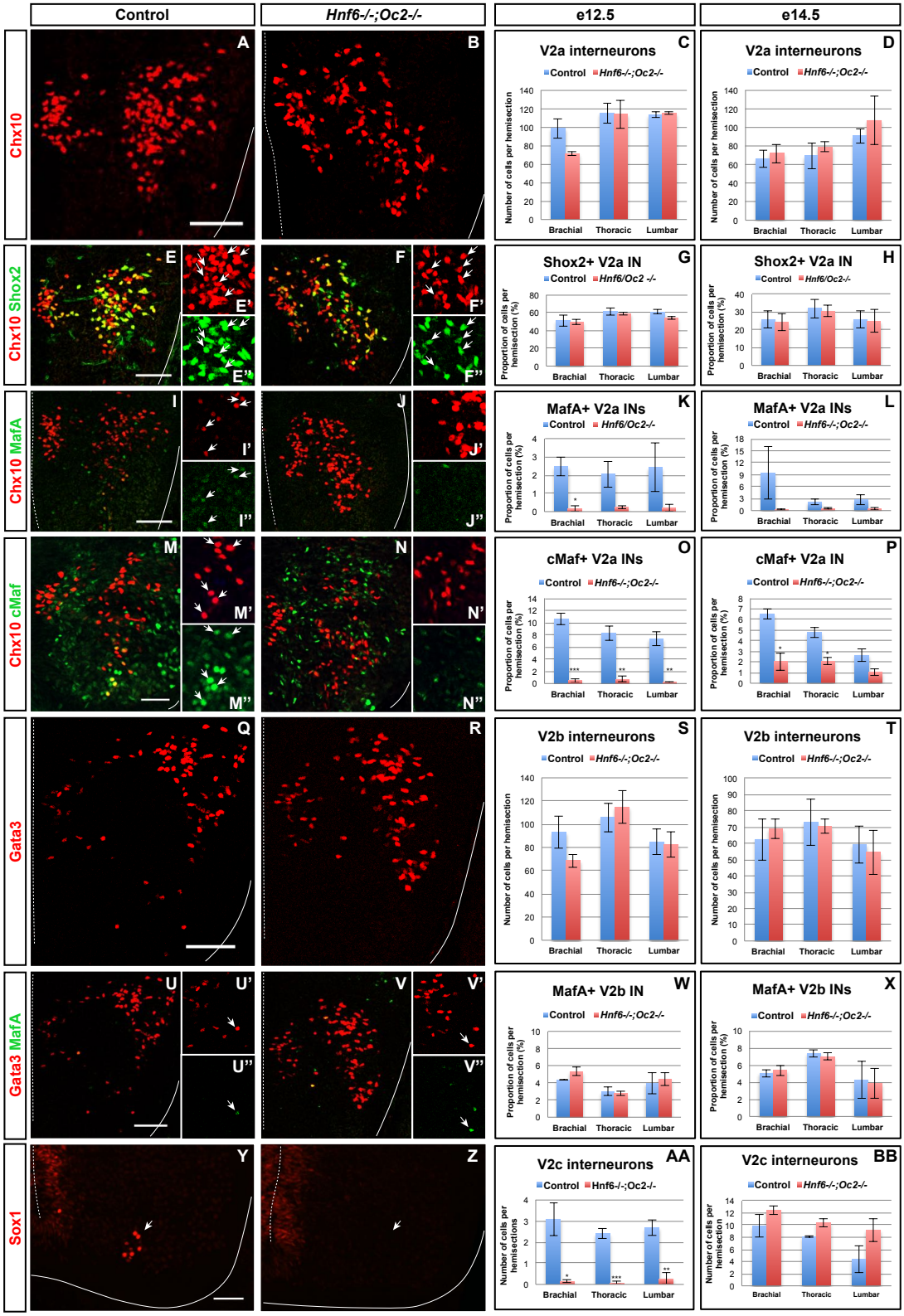

Harris A. et al., Figure 2

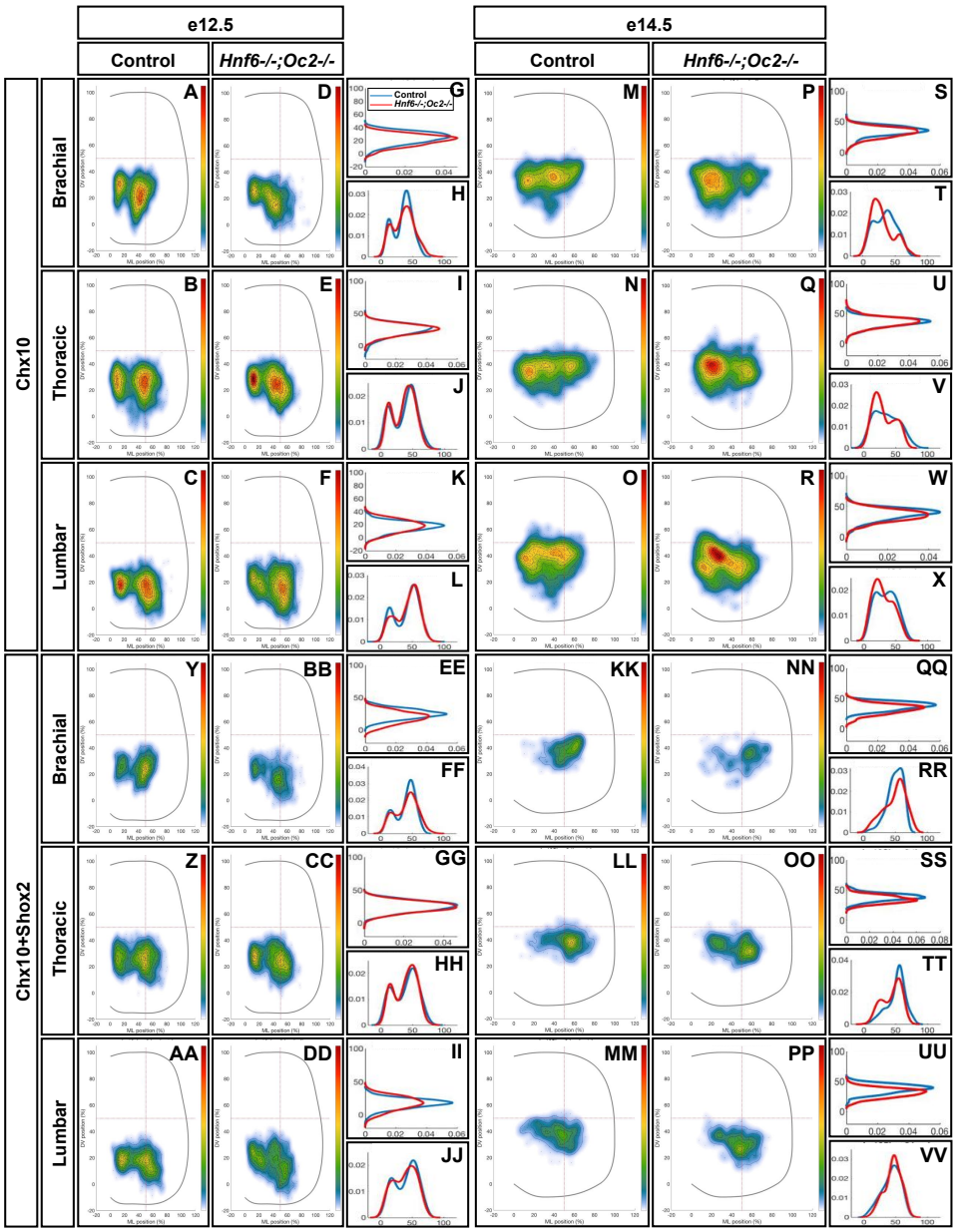

Harris A. et al, Figure 3

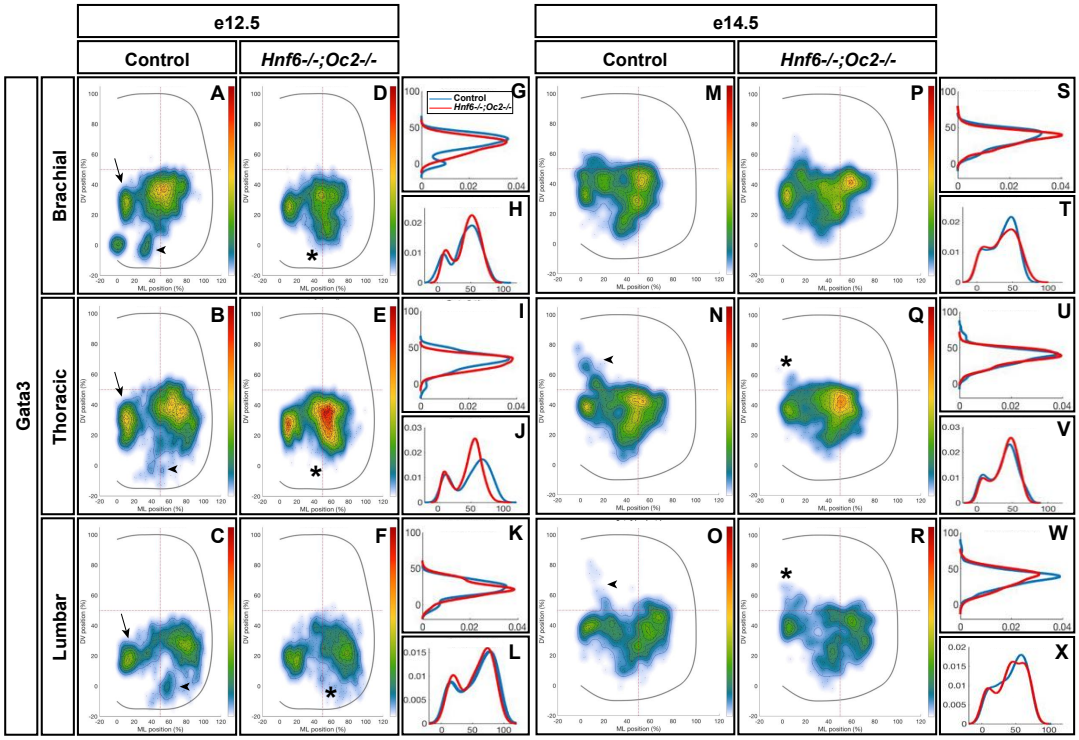

Harris A. et al, Figure 4

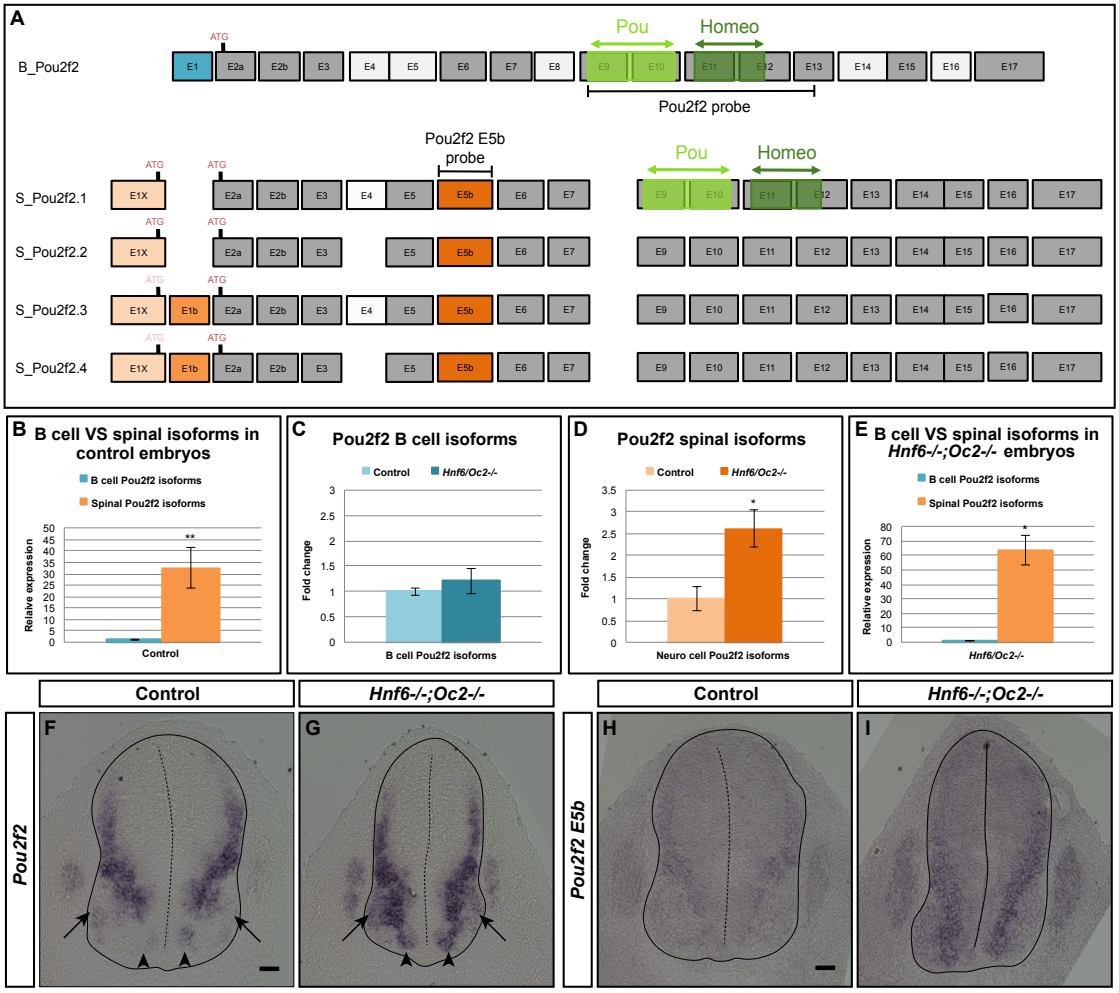

Harris A. et al, Figure 5

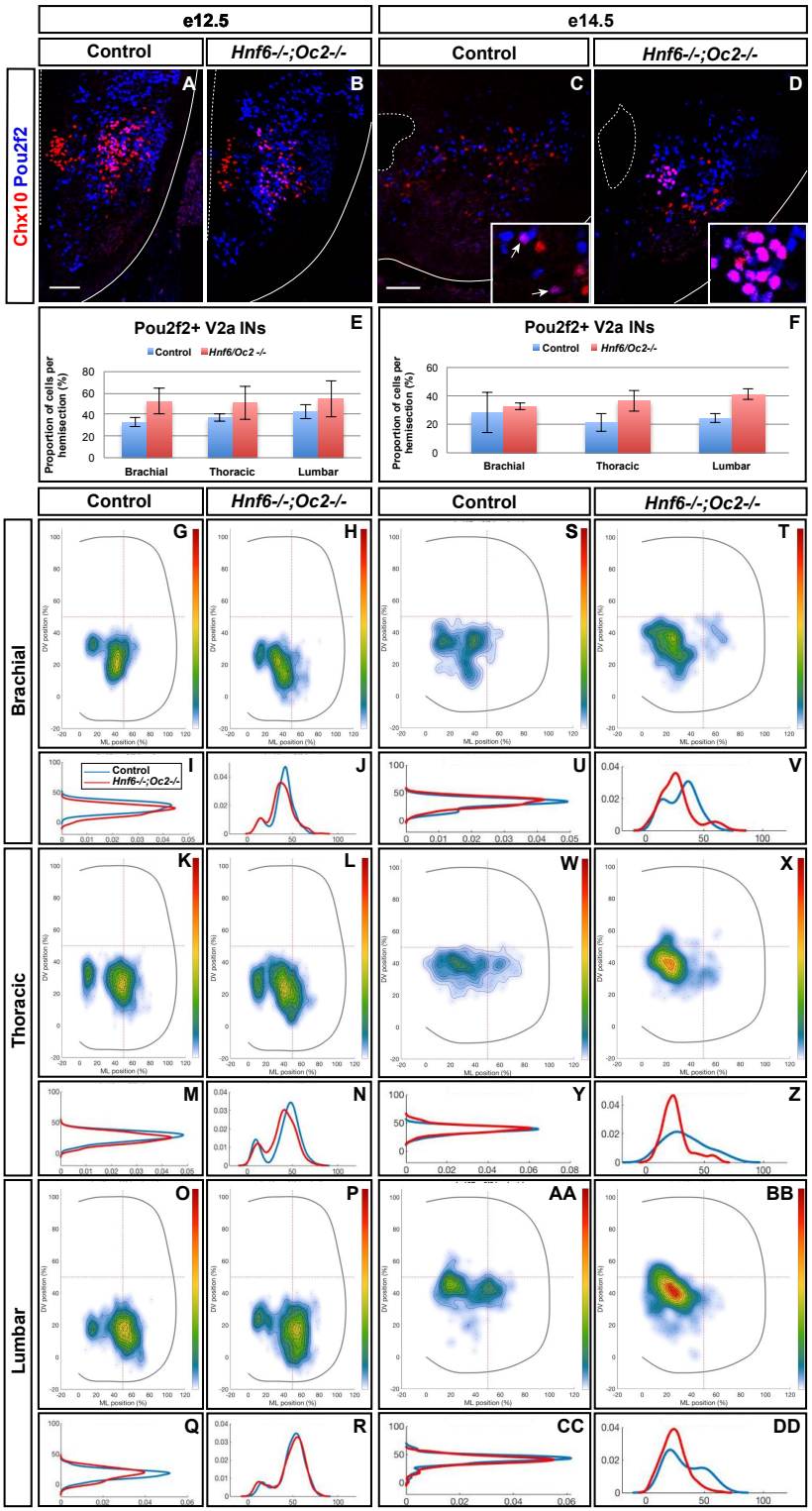

Harris A. et al, Figure 6

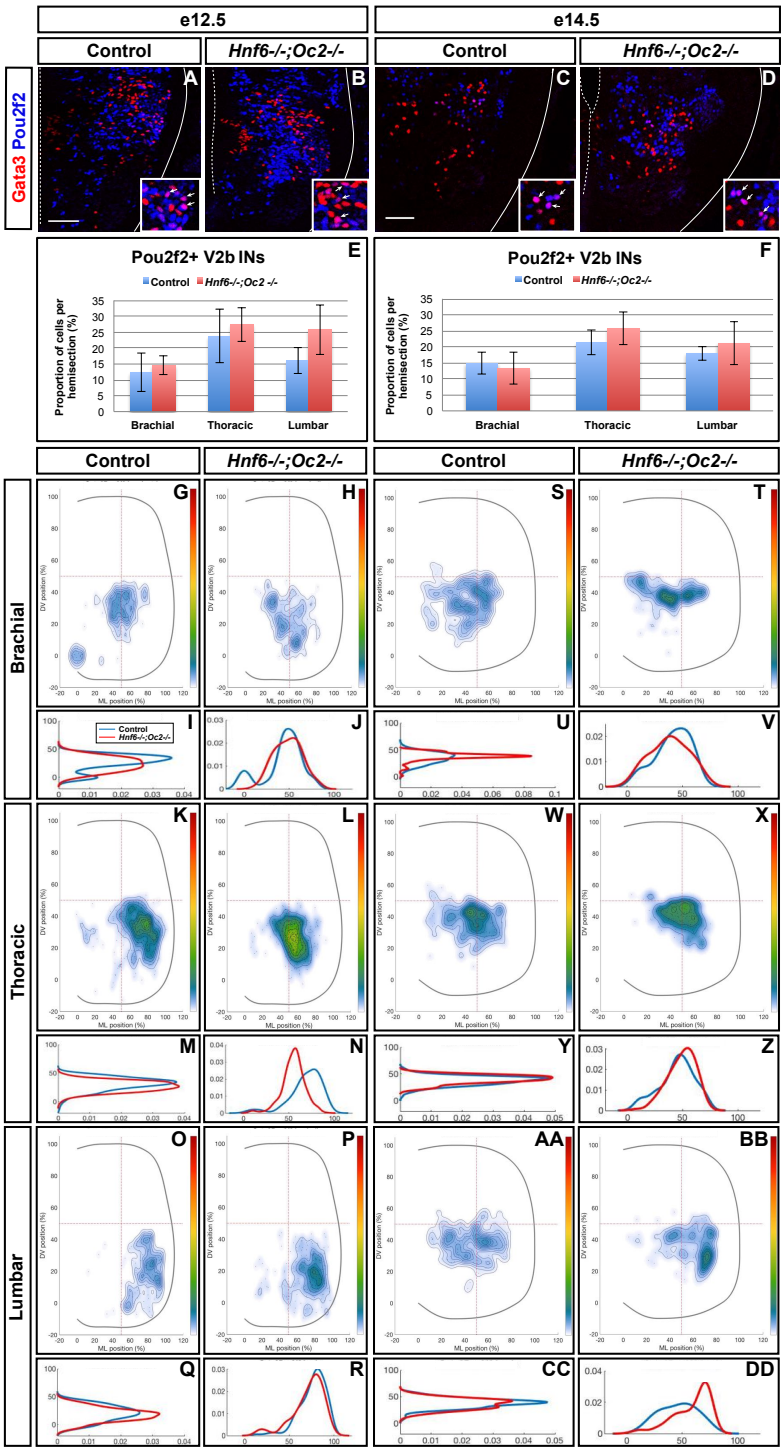

Harris A. et al, Figure 7

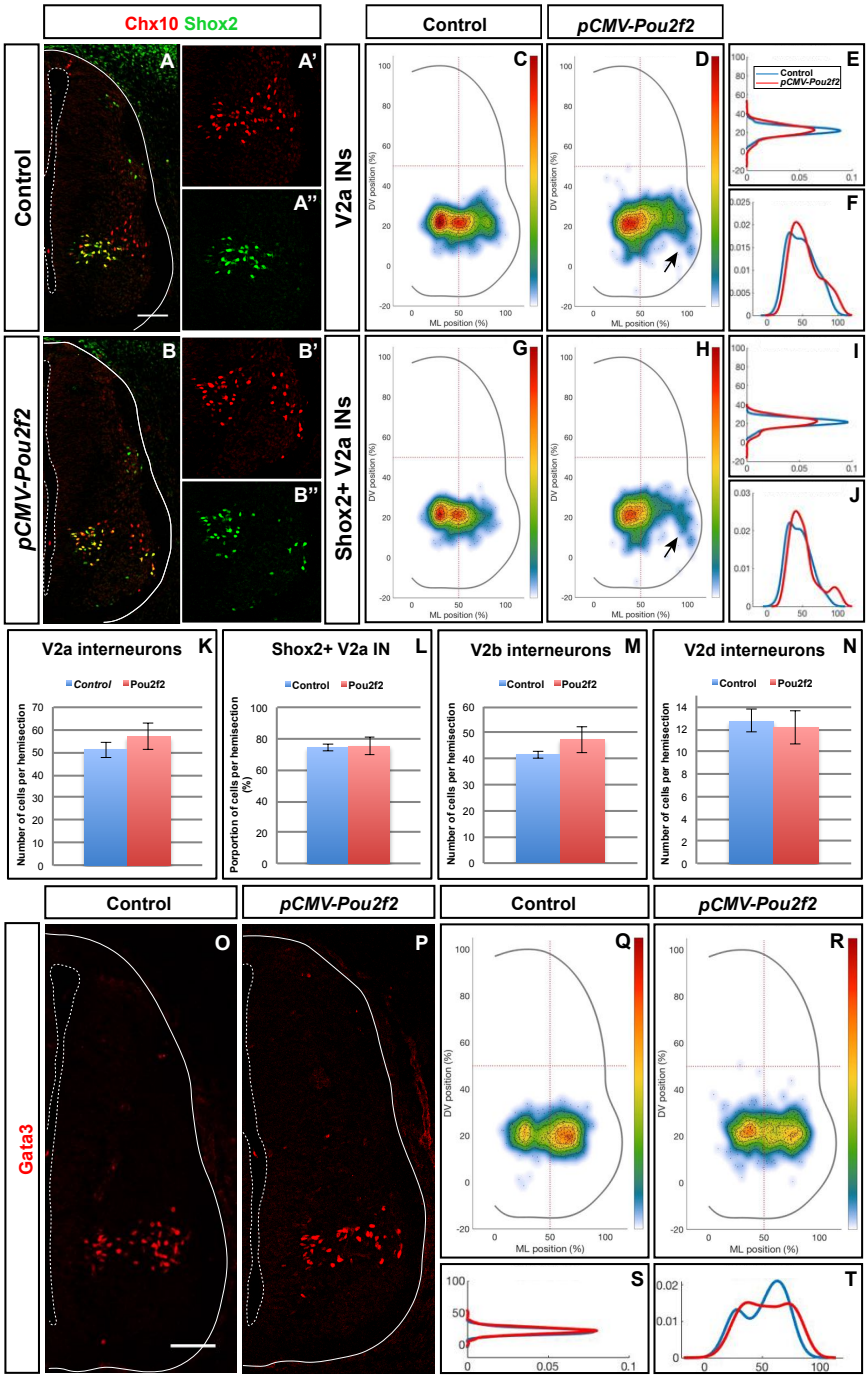

Harris A. et al., Figure 8

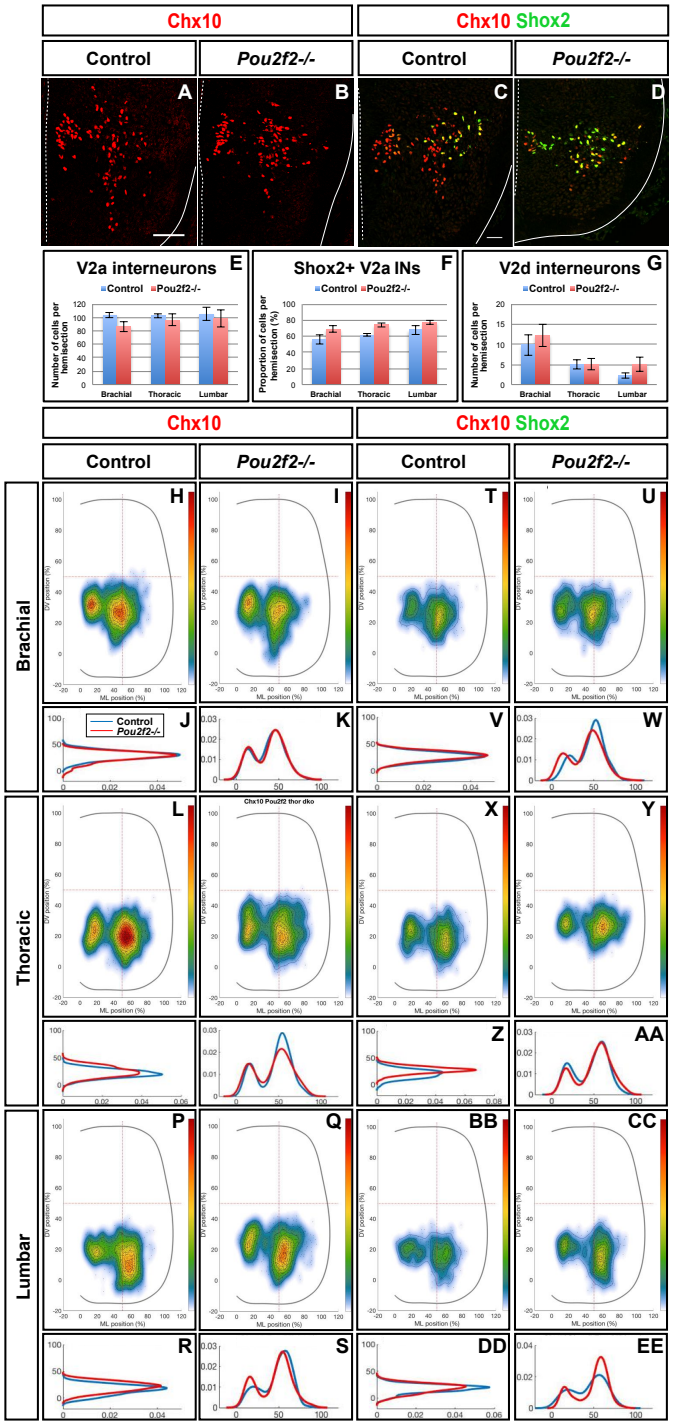

Harris A. et al, Figure 9

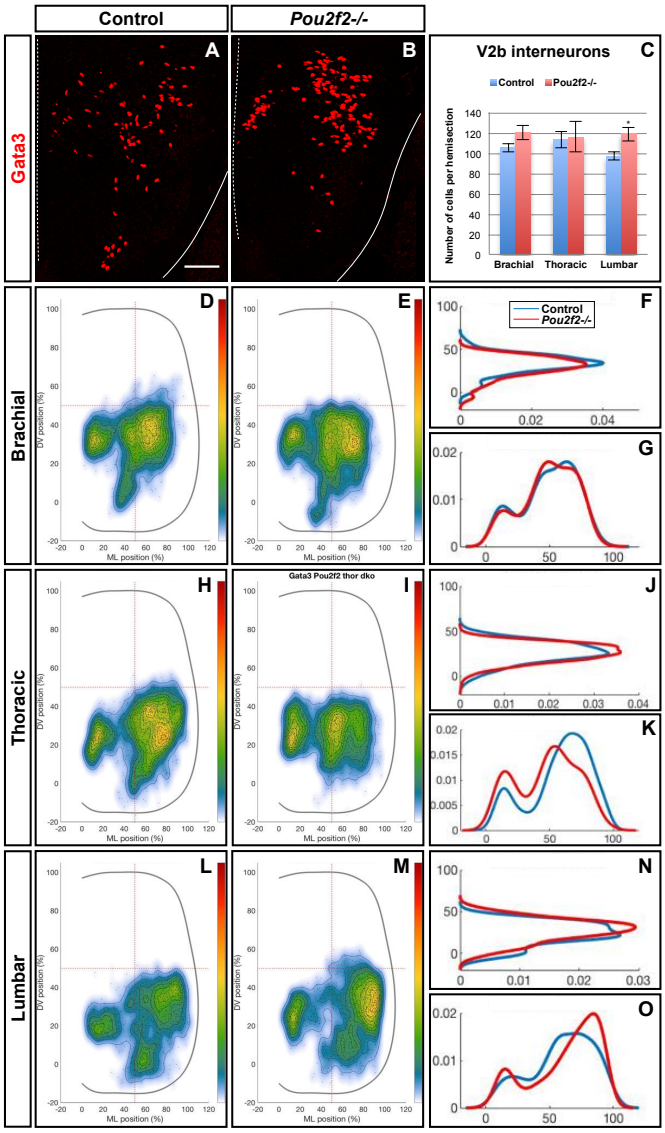

Harris A. et al, Figure 10

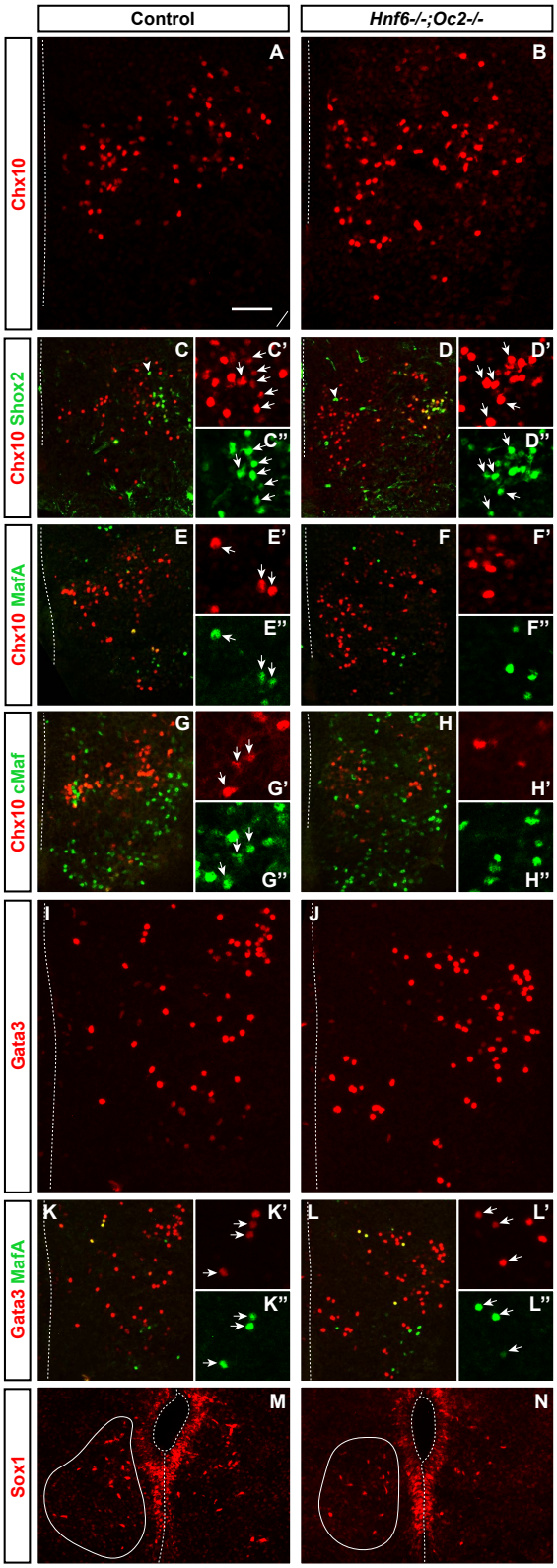

Harris A. et al., Supplementary figure 1

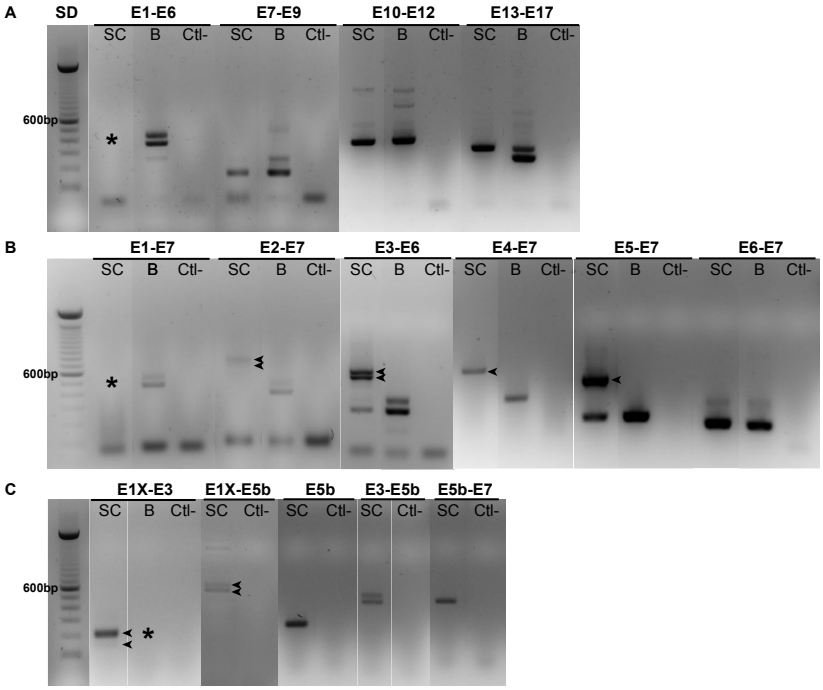

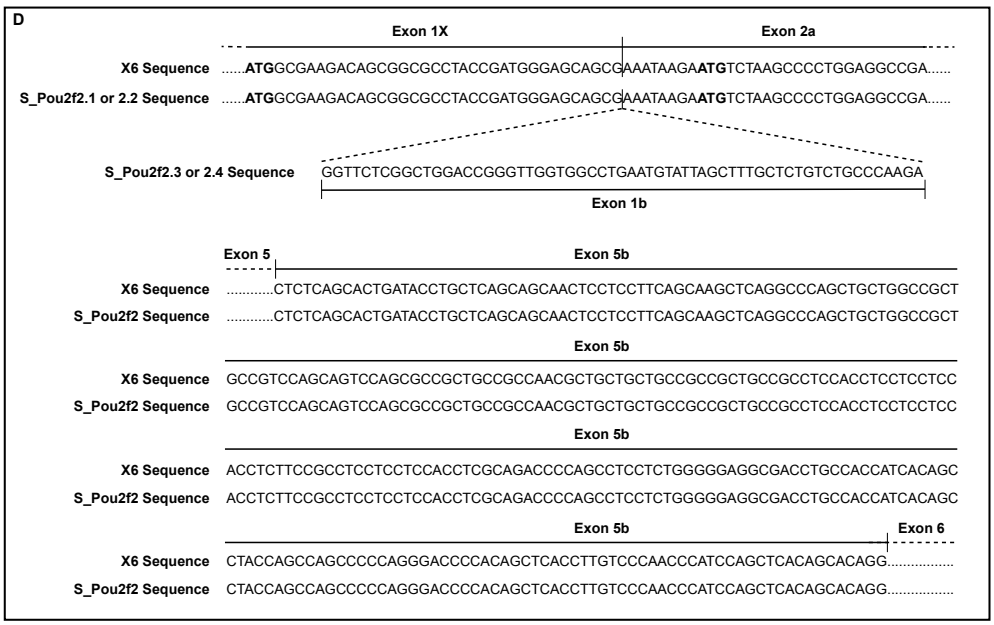

Harris et al., Supplementary figure 2

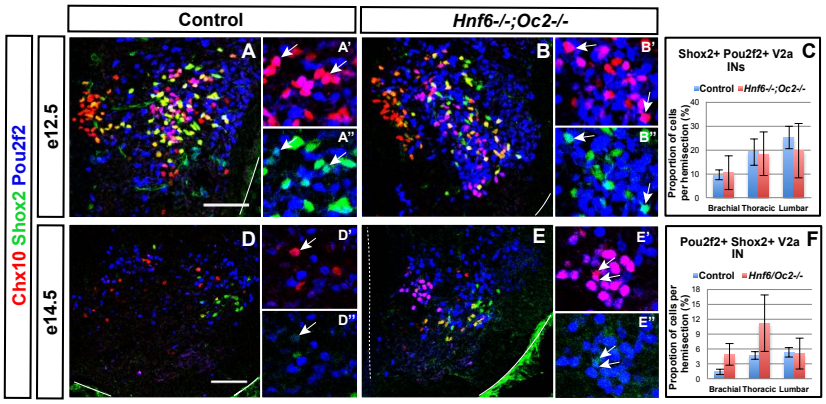

Harris A. et al, Supplementary figure 3

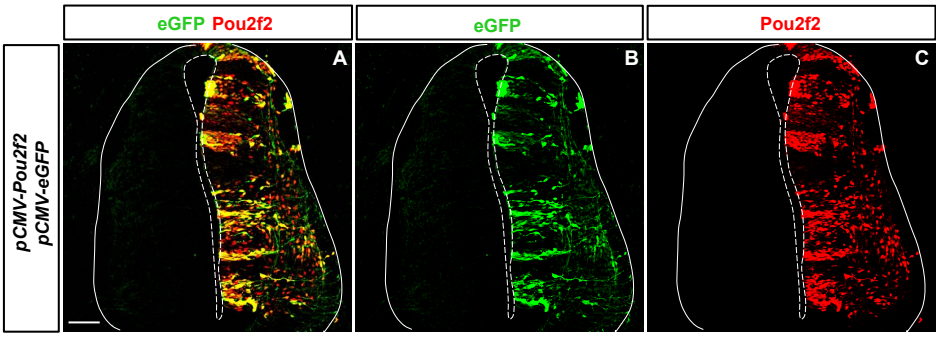

Harris A. et al, supplementary figure 4

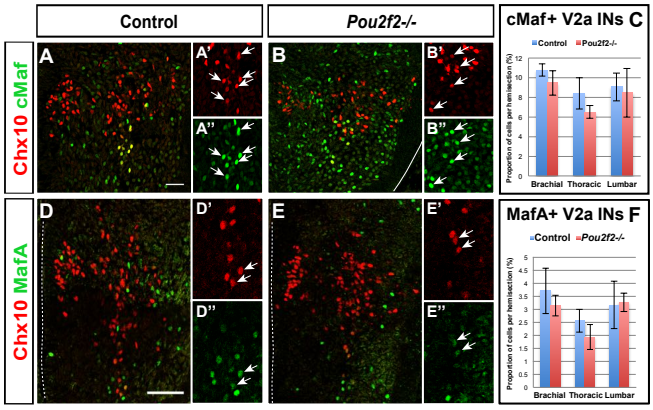

Harris A. et al, Supplementary figure 5

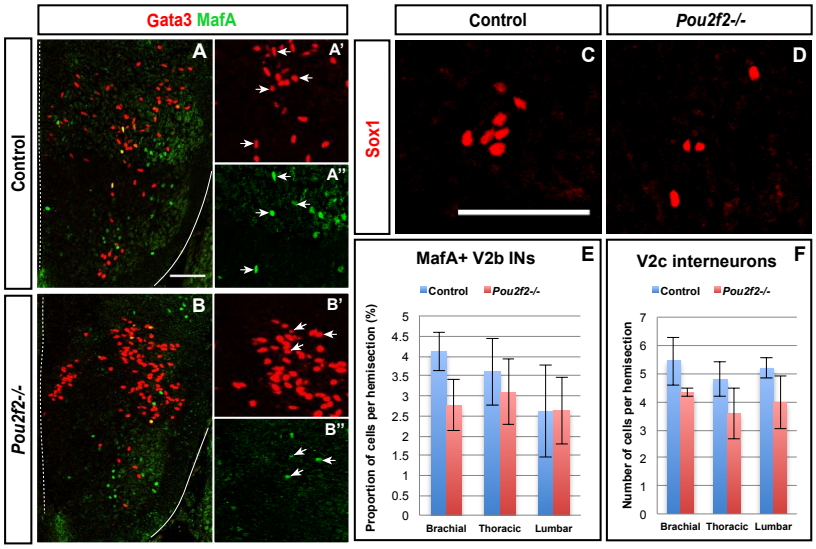

Harris A. et al., Supplementary figure 6